

STUDIES ON THE EFFECT OF TRYPTOPHAN SUBSTITUTIONS IN CHANNEL-
FORMING PEPTIDE: CK₄M₂GLYR

by

JAMMIE LAYMAN

B.A., Kansas State University, 2012

A THESIS

submitted in partial fulfillment of the requirements for the degree

MASTER OF SCIENCE

Department of Biochemistry and Molecular Biophysics
College of Arts and Sciences

KANSAS STATE UNIVERSITY
Manhattan, Kansas

2014

Approved by:

Major Professor
John M. Tomich

Copyright

JAMMIE LAYMAN

2014

Abstract

NC-1007 (CK₄-M2GlyR) (PARVGLGITTVLMTTQSSGSRAK₄) is a synthetic peptide modeled after the second transmembrane segment of the spinal cord glycine receptor's α -subunit, and has demonstrated the capacity to oligomerize to form transmembrane channels with Cl⁻ permselectivity. While studies into the effects of truncation on both CK₄ (C-terminal tetra-lysyl adducted) and NK₄ (N-terminal tetra-lysyl adducted) led to more control over solution aggregation in the NK₄ variant, the work presented explores whether C-terminal sequential substitutions with a tryptophan residue could similarly stabilize the aqueous structure in monomeric form or further define the pore registry in such a way as to promote an increase in ion permeability. Tryptophan was substituted for amino acids in the 18th, 19th, 20th, and 21st positions of the peptide sequence (SSGS, respectively), and changes in aggregation profiles, secondary structure, and channel ion permeability were observed. Synthesized peptides show circular dichroism spectral profiles indicating that the studied tryptophan substitutions did not result in a reduction of the characteristic helicity of the peptide; however, the tryptophan substitution also did little to decrease solution aggregation as demonstrated by comparative studies by reverse-phase high-performance liquid chromatography. All peptides demonstrated channel activity, directly measured by recordings of transepithelial short-circuit current, with profiles that suggest trends in electrostatic interactions and membrane registry relative to substitution position. One peptide in particular, NC-1007 S21W displayed atypical activity, which could not be effectively described by the standard Hill-based model but may be indicative of an ill-defined registry due to the substituted peptide's proximity to another strongly pore-defining residue. Further studies in the effects of sequence modification to channel-forming peptides will elucidate how sequences may be altered to optimize synthetic peptide solubility, resistance to in-solution aggregation, and ability to form selective and permeable ion channels. The understanding gained from this study will improve our ability to develop peptides that could serve as a therapeutic treatment for a number of endogenous channelopathies.

Table of Contents

List of Abbreviations	v
List of Figures	vi
List of Tables	vii
Acknowledgements	viii
Dedication	ix
Preface	x
Chapter 1 - Background and Introduction	1
Ion Channels	1
Ion Flux Across Epithelia	2
The Glycine Receptor (GlyR)	4
An Introduction to Cystic Fibrosis	4
Current Palliative Options and Experimental Therapies	6
Alternative and Experimental Therapies	7
Ion Channel Replacement Therapy	8
M2GlyR-altered sequences	9
Chapter 2 - Materials and Methods	16
Syntheses	16
Cleavage, Deprotection and Characterization	16
Concentration Determination	16
Circular Dichroism	17
Cell Culture	18
Analysis of I_{sc} Data	20
Reverse Phase High Performance Liquid Chromatography (RP-HPLC) Studies	20
UV/Vis Spectrometry	21
Chapter 4 - Results and Discussion	22
Characterization	22
Circular Dichroism	27
RP-HPLC Studies	32
Discussion	36
References	42
Appendix A - Rights and Permissions	52

List of Abbreviations

1-EBIO	1-ethyl-2-benzimidazolinone
CD	circular dichroism
CFTR	cystic fibrosis transmembrane conductance regulator
CK4	carboxy-terminal tetralysl adduct
Dab	diaminobutyric acid
Dap	diaminopropionic acid
DIEA	Diisopropylethylamine
DMEM	Dulbecco's modified Eagle's medium
EDTA	ethylenediaminetetraacetic acid
F-12	Ham's F-12 nutrient mixture
FBS	fetal bovine serum
Fmoc	9-fluorenylmethoxycarbonyl
GlyR	glycine receptor
HBTU	2-(1H-benzotriazole-1-yl)-1,1,3,3-tetramethyluronium hexafluorophosphate
HOBt	N-Hydroxybenzotriazole
HPLC	high performance liquid chromatography
ICRT	ion channel replacement therapy
I_{MAX}	maximal short circuit current
I_{sc}	short circuit current
$K_{1/2}$	concentration at half maximal short circuit current
LGIC	ligand-gated ion channel
M2GlyR	peptide modeled after the second transmembrane segment of the glycine receptor
MALDI-TOF	matrix-assisted laser desorption ionization time of flight
MDCK	Madin-Darby canine kidney
MS	mass spectrometry
MTS	methanethiosulfonate
nAChR	nicotinic acetylcholine receptor
NK4	amino-terminal tetralysl adduct
NMP	N-methylpyrrolidone
NMR	nuclear magnetic resonance
PBS	phosphate-buffered saline
PDB	Protein Data Bank
P/S	penicillin/streptomycin
SDS	sodium dodecyl sulfate
SEM	standard error of the mean
TFA	trifluoroacetic acid
TFE	2,2,2-trifluoroethanol
TM	transmembrane
WT	wild type

List of Figures

Figure 1.1: Association profile of CK ₄ - and NK ₄ -M2GlyR p27	11
Figure 1.2: Cross-Linked M2GlyR Truncated Peptides	12
Figure 1.3: Activity of Truncated M2GlyR Segments NK ₄ - and CK ₄ -M2GlyR.....	13
Figure 1.4: Peptide concentration dependence on I_{SC} in MDCK monolayers	14
Figure 4.1 MALDI-TOF spectral profiles for experimental peptides.....	27
Figure 4.2: Circular Dichroism profiles of NC1007 W-substituted peptides	28
Figure 4.3 Course of a typical Ussing chamber experiment.....	29
Figure 4.4: Concentration-dependence of peptide on peak ΔI_{sc} in MDCK epithelial cells	30
Figure 4.5: HPLC chromatographs of tryp-substituted peptides	35
Figure 4.6 (opposite): Helix Wheel models of w-substituted NC1007 variants.....	41
Figure 4.7 UV/Vis spectrophotometric profiles.....	41

List of Tables

Table 4.1 Common name, sequence, and molecular mass of experimental w-substituted variants of NC1007.....	22
Table 4.2 Kinetic Parameters of W-Substituted NC1007 Peptides	31

Acknowledgements

First and foremost, I would like to thank my principal advisor, Dr. John M. Tomich for his unending help and support. Not only did he serve as an outstanding advisor and academic mentor, but also as a counselor, confidant, guide, and friend both professionally and personally. I am eternally grateful to have had such a wonderful character in my life, and I would not be who I am today without his infinite support, faith, and guidance. Thank you, John.

I would also like to thank committee members Dr. Bruce D. Schultz and Dr. Timothy Durrett for their help, advice, criticism, and perhaps most notably, their constant understanding in dealing with the struggles of a philosopher in the science arena. I have learned so much, and over the few years I have truly fallen in love with the wonderfully empirical world that is biochemistry. Thank you for having faith that even a humanities graduate can be learn and be enriched by the hard sciences. I will forever be grateful for your advice and patience!

Furthermore, I would like to thank fellow Tomich laboratory members Dr. Yasuaki Hiromasa, Benjamin Katz, Pinakin Sukthankar, Adriana Avila-Flores, Susan Whitaker, and undergraduate assistant Kaitlyn Gerwick, as well as Schultz laboratory members Lin-Hua (Florence) Wang, Quian Wang, and Fernando Pierucci-Alves for all of their guidance, assistance, and sometimes simply wonderful company. The experience would truly not be the same without all of you.

Finally, and perhaps most importantly, I'd like to thank my loving family and friends for their continued advice and support. I love you all so much.

Dedication

To the late N.L. You are forever missed.

Preface

“Wisdom begins in wonder” -Socrates

Chapter 1 - Background and Introduction

Ion Channels

Ion channels are protein complexes that allow for the movement of ions across cellular membranes. Ion channels often employ gating mechanisms dependent on ligands or voltage, and are defined by a number of characteristics of the pore that they form, including conductance, length, and dielectric constant (Futaki 1998; Stoikov et al., 2003). Ion channels are generally composed of proteins, some of which assemble to form a permeable pore. Pore size and residue type at or near the narrowest part of the channel, known as the selectivity filter, affect which ions can permeate through the channel (Ashcroft, 2000; Hille, 2001).

Amino acid residues can be positively or negatively charged (and therefore hydrophilic), uncharged but polar, or non-polar. Hydrophobic nonpolar residues tend to comprise the transmembrane domain of the protein, while hydrophilic residues tend toward the extra- or intracellular space. Certain amino acid residues have somewhat predictable effects on the pore structure. For example, proline, due to its cyclic side-chain, displays notable conformational rigidity, and is frequently found at the terminus of the peptide's α -helix, and therefore often defines the boundary of the transmembrane domain in membrane-spanning peptides and proteins (Ashcroft, 2000). Serine, threonine, and tyrosine can be phosphorylated to induce a negative charge, potentially altering the structure and function of the peptide or channel through this change in electrostatic interactions. Extracellular residues also may undergo glycosylation, adding mass that may have an effect on structure or function of the channel. It is generally assumed that transmembrane segments are often α -helical in secondary structure, comprised of 16-20 amino acids, and often contain many alanine, glutamate, methionine, or leucine residues, which have a greater propensity for the formation of α -helical structures.

This opening and closing mechanism of ion channels is known as gating, and can be driven by voltage changes or covalent modification of the peptide or protein. Single channel recordings can determine the channel's opening and closing rates as well as conductance. The ratio of the time the channel is open to the total duration of the recording is known as the open probability, and can be used to calculate macroscopic current from single-channel current data if the number of channels and single channel current is known. This value can be obtained using the following equation:

$$I = i_n P_o$$

Where I is macroscopic current; i , single-channel current; n , the number of active channels; and P_o , the probability of any given channel being open.

The majority of channels have a single conductance state, meaning that during times spent open, given that the membrane potential is constant, the amplitude of current through the channel is consistent. In some cases, however, certain channels can demonstrate multiple conductance states. Current through a single channel varies with intra- and extra-cellular concentrations of present ion species, membrane voltage potential, and solubility.

Electrochemical gradients determine the direction of movement through the pore, as well as flow rate (Ashcroft, 2000).

Ion Flux Across Epithelia

A number of different ions flow into and out of an epithelial cell, impacting the membrane potential that serves as the driving force for ion movement. In order to understand Cl^- transport through CFTR or M2GlyR peptides, it is important to understand the complex interplay of other transporters that affect net driving forces.

Na^+/K^+ ATPase (a.k.a. Na^+/K^+ pump) contributes substantially to cellular energy expenditure, accounting for roughly 2/3 of ATP utilization. It is electrogenic, moving 3 Na^+ and 2 K^+ against their concentration gradients (out of and into the cell, respectively). This plays a fundamental role in maintaining cellular potential and the electrochemical gradients that serve as the driving force for the secretion of other ions, such as Cl^- (Skou, 1998). Similarly, K^+ channels such as TWIK (two-pore domain weak inward rectifying K^+ channel) related channels, such as TASK (TWIK-related acid-sensitive K^+ channel) and TREK (TWIK-related K^+ channel) and an abundance of Ca^{2+} activated K^+ channels play a key role in maintaining voltage potential of the epithelial cell. In order to maintain polarization of the cellular resting potential, positively charged ions must be pumped out of the cell at a steady rate, counterbalancing the influx of positively charged Na^+ . This efflux of K^+ thereby repolarizes the cell so as to promote anion efflux. The $\text{Na}^+/\text{K}^+/\text{2Cl}^-$ cotransporter (epithelial isoform NKCC1) mediates the uptake of 2 Cl^- ions into the cell, driven by its coupled influx with one K^+ and one Na^+ ion (Frizzell & Hanrahan, 2012; Wills et al., 1996). In the typical epithelial cell, the concentrations of predominant ions Na^+ , K^+ , Ca^{2+} , Cl^- , and HCO_3^- play the most significant role in ion transport.

Diffusive forces will generally drive ions to move down a gradient from high to low concentration. However, in biological systems electrical gradients can oppose those of diffusion, and depending on the system, there exists a certain equilibrium potential at which these forces are perfectly opposed such that there is no net ionic flux. Ohm's law relates the electrical driving

forces and movement for ions current through a conductive pathway, and is defined in terms of current (I), conductance (G) and voltage (V), such that:

$$I = G \cdot V$$

The Nernst equation defines this voltage with respect to the ion's valence and transmembrane concentration gradient. The Nernst equation can be expressed as:

$$E_x = (RT/(z)F) \cdot \ln([X]_{\text{ext}}/[X]_{\text{int}}) \text{ or alternatively,}$$

$$E_x = (2.3RT/(z)F) \cdot \log([X]_{\text{ext}}/[X]_{\text{int}})$$

Where V_x is the equilibrium potential for the given ion; R is the universal gas constant, 8.314 J/(mol*K); T is temperature in Kelvin (assumed at 310K for body temperature); z is ion valence (negative for anions, positive for cations); F is Faraday's constant (9.6484×10^4 coulombs/mol); X is the given ion being evaluated (e.g. Cl⁻) and its extracellular ($[X]_{\text{ext}}$) and intracellular ($[X]_{\text{int}}$) concentrations.

The Nernst equation, however, is limiting in that it can only express the equilibrium potential relative to the intra- and extra-cellular concentrations of a single ion. In actuality, however, the membrane is permeable to multiple ions that contribute to the electrochemical gradient that drives ion flux. In the case of multiple ion transport, equilibrium potential is reached when the current relative to all ions in flux rests at zero. The Goldman-Hodgkin-Katz (GHK) equation can be used to calculate the membrane potential of a cell that is permeable to more than a single ion species, and is given as:

$$V_m = \frac{RT}{F} \ln \left(\frac{p_K [K]_o + p_{Na} [Na]_o + p_{Cl} [Cl]_i}{p_K [K]_i + p_{Na} [Na]_i + p_{Cl} [Cl]_o} \right),$$

Where V_m is membrane potential; R, the universal gas constant; T, temperature in Kelvin; F, Faraday's constant; p_x , the permeability of a given ion (in cm/sec); $[X]_o$, the extracellular, and $[X]_i$, the intracellular concentrations of the given ion; and K (K⁺), Na (Na⁺), and Cl (Cl⁻), the ions in question for epithelial membranes.

The Glycine Receptor (GlyR)

Cl⁻ channels play functional roles in transepithelial transport as well as membrane excitability and cellular pH modulation. At least three distinct families of Cl⁻ channel exist (Jentsch and Günther, 1997): voltage-gated channels, CFTR-like channels, and ligand-gated channels such as those activated by opened by GABA and glycine. The binding of the neurotransmitter glycine to the receptor opens the pore and allows for Cl⁻ secretion. The glycine receptor, like most ion channels, is composed of several subunits that assemble to form a selective pore. The channel pore is formed at the center of the cluster that consists of both α and β subunits. A variant containing only α -subunits of GlyR combine to form homopentameric pores that expressed functionality in *Xenopus* oocytes (Schmeiden et al., 1989). The fact that a single M2 sequence can form a chloride channel made this an obvious choice for further investigations.

An Introduction to Cystic Fibrosis

Epithelia, composed of numerous tightly packed cells, serve as barriers that employ diverse channels and transporters to regulate the movement of solutes and solvents into and between different body compartments. Epithelial barriers protect organs and the body as a whole from unregulated penetration of harmful substances and also serve to sustain the necessary concentrations of various chemicals within those compartments. Improper function of the channels that contribute to solute and solvent transport can lead to illness or death.

Cystic fibrosis is a recessive autosomal genetic channelopathy (Becq, 2010); the result of dysfunctional CFTR, or cystic fibrosis transmembrane conductance regulator, which contributes to the permeation of anions across epithelial membranes (Zhang, 2000). CFTR is encoded by its eponymous gene, and is itself indirectly regulated by cyclic adenosine monophosphate (cAMP) (Sheppard and Welsh, 1999; Davis 2006). The protein is composed of two nucleotide-binding domains, two membrane-spanning domains, and a regulatory domain, which contains sites that can be phosphorylated by protein kinase A (Riordan, 2008; Devidas and Guggino, 1997; McCarty, 2000; Zhang et al., 2000). Protein kinase C has also been reported to modify CFTR function (Jia et al., 1997). CFTR is an adenosine triphosphate (ATP) binding cassette transporter, a member of a family of transmembrane proteins that use ATP as an energy source in carrying out their respective functions (Higgins, 1995). CFTR is the only member of this superfamily that acts as an ion channel, primarily serving to facilitate anion transport across epithelia throughout the body (Quinton, 1999; Davis 2006).

Mutations responsible for malfunctions in CFTR that lead to cystic fibrosis are categorized into five classes relative to their respective mechanisms of disruption (Pilewski and Frizzell, 1999). Classes 1 and 2 lead to disease across multiple organs, most notably pancreatic insufficiency, male infertility, bowel obstruction, and progressive lung disease (Rowntree and Harris, 2003). Class 1 comprises all mutations that result in abnormal biosynthesis and/or disrupted translation of CFTR. Class 2 contains mutations that affect the folding and trafficking of the protein. The most common mutation to CFTR, $\Delta F508$, which represents a deletion of phenylalanine at position 508 of the protein, is a class 2 mutation. $\Delta F508$ CFTR is recognized by the cell as a defective protein, and is endosomally degraded before it can form a channel in the cell membrane (Mall et al., 2004; Kopito, 1999; Pilewski and Frizzell, 1999). Class 3 is virtually indistinguishable from class 1 and class 2 type mutations with respect to its resulting symptoms in the lungs and pancreas (Pilewski and Frizzell, 1999; Rowntree and Harris, 2003). However, this class includes mutations that affect regulation of channel gating (Pilewski and Frizzell, 1999) and is typified by the well-characterized G511D mutation. Classes 4 and 5 of CFTR-disrupting mutations lead to partial function in CFTR channel activity at the cell membrane. With class 4 mutations, an otherwise normally developed CFTR protein forms a channel that exhibits decreased gating or transport ability of chloride relative to its fully-functional counterpart. Class 5 mutations characterize those that result in the alternative splicing of mRNA sequences, which leads to an alternate transcript, and therefore a reduction in expressed CFTR. Class 5 mutations can result in pancreatic disease and congenital bilateral absence of the vas deferens (CBAVD; Pilewski and Frizzell, 1999; Rowntree and Harris, 2003).

Compromised CFTR function can cause a wide variety of maladies by way of insufficient ion transport in a number of corporeal systems, including the sweat glands, pancreas, and airways. Pulmonary disease is perhaps the most widely recognized symptom of cystic fibrosis that results from recurrent or chronic bacterial infection by *Pseudomonas aeruginosa*, *Staphylococcus aureus*, *Burkholderia cepacia*, and *Haemophilis influenza* (Rowe et al., 2006). These bacteria thrive in the thick, sticky mucus that accumulates due to reduced fluid secretion in the lungs and remains uncleared from the airways (Quinton, 1999; Planells-Cases and Jentsch, 2009). Activation of nuclear factor kappa B by neutrophils and macrophages leads to inflammation and scarring, which is typical of the disease (Rowe et al., 2006). Furthermore, studies suggest also that inflammatory response regulation may be impaired by defective CFTR (Pilewski and Frizzell, 1999). The thick, viscous mucus that supports the infection is the result of leukocyte apoptosis and abnormal, dehydrated mucin glycoproteins that fail to fully unfold when secreted (Davis, 2006). Not only does the fluid on the surface of the airways aid in the hydration

of the system and facilitate the clearance of mucus, it also contains neutrophils and macrophages that help reduce infections (Tarran, 2004).

In addition to lung infections and bronchiectasis, mutations of *CFTR* and dysfunctional CFTR protein can result in a wide range of symptoms, due in part to its role in regulating concentrations of Cl^- and bicarbonate (HCO_3^-), and subsequently, concentrations of counter-ions and fluid volume. Normally Na^+/K^+ -ATPase moves Na^+ out of the cell from the basolateral membrane, creating a driving force for apical Na^+ uptake. Adrenaline stimulates receptors that increase cellular cAMP, releasing sweat from the duct and increasing the uptake of extracellular salts. In CF epithelia, however, inadequate Cl^- uptake leads to depolarization as sodium is still absorbed into the epithelium. This ultimately leads to a reduction in driving force for continued sodium absorption, resulting in the excess salt in human sweat, which serves as the basis of the common “sweat test” for CF (Ashcroft, 2000; Rowe et al., 2006). The transport of HCO_3^- can also be impacted by abnormal CFTR, through which it permeates, or indirectly by way of the effect of Cl^- concentration imbalances on the $\text{Cl}^-/\text{HCO}_3^-$ exchange transporter present in the lungs and ducts of the pancreas (Kim and Steward, 2009). Impaired transport of Cl^- in biological epithelia is a direct result of malfunctioning CFTR, and often results in abnormal or reduced fluid secretion (Welsh, 1987; Li et al., 1989, Anderson et al., 1992; Smith et al., 1994; Zhou et al., 2002).

Current Palliative Options and Experimental Therapies

The majority of present therapies for cystic fibrosis are palliative in nature. Patients suffering from cystic fibrosis-related diabetes are generally given insulin to compensate for the resistance and decreased production of the hormone. Dietary supplements, such as Yasoo Health Inc’s compound, AquADEKs® restore necessary vitamins deficient in those with the disease and have been shown to reduce several cystic fibrosis associated pulmonary symptoms (Sagel et al., 2011). The USFDA has approved several therapies for the replacement of pancreatic enzymes, which aid in vitamin and nutrient absorption. These include Zennen® (Eurand Pharmaceuticals), Creon® (Abbott Laboratories) and Pancreaze™ (Ortho-McNeil Pharmaceutical). Several others are still in the pipeline, but require additional clinical trials for approval (Lowry, 2011). Insulin supplements are used to restore function for those who suffer from cystic fibrosis related diabetes.

Antibiotics and anti-infectives such as Aztreonam-based Cayston® (Gilead Sciences), tobramycin-based TOBI® are used to target *Pseudomonas aeruginosa*, a common bacteria in CF airways, and have been reported to improve lung function (Cheer et al., 2003). Antibiotics can be

administered via a wide range of delivery systems (Gibson et al., 2003). Azithromycin (Pfizer, Inc.) has also been explored as an antibiotic for CF patients. While it initially showed great promise in reducing infections of *Pseudomonas aeruginosa* (Saiman et al., 2003), more recent studies suggest that prolonged use may contribute to heart disease (Ray et al., 2012) and chronic infection by other bacteria (Renna et al., 2011). Anti-inflammatories fight the pulmonary inflammation that leads to fibrosis and a decrease in lung function in CF patients. Twice-daily ibuprofen was shown to slow the rate of deterioration of the pulmonary systems of those with CF (Konstan et al., 1995). KB001 (Kalobios Pharmaceuticals) moderates virulence factors of *Pseudomonas aeruginosa* that play a role in inflammation (Baer et al., 2008).

A number of approaches target viscous pulmonary mucus to address CF symptoms. These include airway rehydrating agents, which work to flush extant mucus in the lungs and promote expectoration (Pettit and Johnson, 2011) and mucolytics, which reduce mucosal viscosity. Dornase alfa-based Pulmozyme® (Genentech) is a recombinant human deoxyribonuclease, which acts to decompose mucus-thickening DNA, and has been shown to reduce infection rates and increase lung function in those with CF (Fuchs et al., 1994); Moli1901 (Lantibio Pharmaceuticals) works by Cl^- conductance via alternate channels to improve lung function (Grasemann et al., 2007); and GS9411 (Gilead Sciences) acts to inhibit the absorption of sodium via epithelial Na^+ channels (ENaC) (Sears et al., 2011; clinicaltrials.gov). A mist of nebulized hypertonic saline was shown to improve pulmonary function, presumably by safeguarding healthier airways from continued infection (Elkins et al., 2006; Donaldson et al., 2006), and inhaled mannitol acts by osmosis to increase airway hydration (Jaques et al., 2008; Bilton et al., 2011).

Alternative and Experimental Therapies

Several experimental therapies demonstrate potential as alternatives to palliative treatment and aim to replace dysfunctional CFTR or restore function to mutated forms. PLASmin® compacted DNA (Copernicus Pharmaceuticals) is a gene therapy that avoids some common difficulties presented by viral vectors through the use of polycation-condensed DNA (which condenses DNA by roughly 1000x), and is capable of membrane permeation (Chen et al., 2007). Intra-nasal application showed tolerability and increased function, but evidence of gene expression was absent (Konstan et al., 2004).

Ivacaftor (Kalydeco; VX-770; Vertex Pharmaceuticals) is noted as one of the first FDA-approved non-palliative therapies for CF. VX-770 decreases the high closing rate of CFTR channels resulting from the G551D mutation. VX-770's potentiating action requires no ATP, but depends on phosphorylation (Eckford et al., 2012). It has also been shown to improve pulmonary

function and normalize Cl^- levels in human sweat (Sheridan, 2011). Ivacaftor has also been used in combination with Lumacaftor (VX-809; Vertex Pharmaceuticals), which corrects trafficking of CFTR in CF patients with common mutation ΔF508 (Thibodeau et al., 2010). As with the G551D mutation, VX-770 maintains the pore's open conformation (Pollack, 2011; and <http://investors.vrtx.com/releasedetail.cfm?releaseid=583683>). This combination therapeutic has recently passed all clinical trials, and Vertex will be submitting a new drug application to the USFDA by the end of the year for potential approval in 2015 (<http://investors.vrtx.com/releasedetail.cfm?ReleaseID=856185>).

Small-molecule therapeutic, Ataluren® (PTC Therapeutics) restores full-length CFTR from those harboring harboring nonsense mutations. Clinical trials demonstrated increased ion transport in nasal epithelia (Wilschanski et al., 2011; and http://www.ptcbio.com/3.1.1_genetic_disorders.aspx), but there is debate about the credibility of the assay in these trials (Auld et al., 2010; Peltz et al., 2009).

Ion Channel Replacement Therapy

The subsequent experiments explore what is believed to be a more straightforward and optimizable approach to CFG therapy: the use of synthetic peptide channels as a substitute for naturally produced CFTR. This method of ion channel replacement therapy avoids many pitfalls of gene therapy, including difficulty with viral vectors, transformation, subsequent functionality of the protein. The aim is to develop easily deliverable, anion selective pore-forming peptides with maximal ability to regulate ion flow and minimal antigenic effects.

This laboratory's aim has long been the production and optimization of synthetic peptides capable of forming ion-penetrable pores modeled after an ion channel found in the glycine receptor of the spinal cord. These peptides, classified as M2GlyR peptides, are modeled after the second transmembrane segment (M2) of the glycine receptor alpha-subunit (GlyR), which was initially characterized by Reddy et al. (1993). Those studies demonstrated anion-selective transport across lipid membranes, showing similarity to the native Glycine receptor. This model has served as the foundation for subsequent studies on various permutations of the original M2GlyR sequence (PARVGLGITTVLMTTQSSGSRA; from amino acid 250-272 of GlyR). Further studies explored the effects of addition, elimination, and substitution of amino acids in the sequence on structure, channel-forming ability, and subsequent ion conduction. Numerous CFTR transmembrane segments (M1-6; M10-12) have been implicated as playing a role in the formation of the Cl^- selective pore (Montal, et al., 1994; Zhang et al., 2000; Linsdell, 2006), and the channel's selectivity filter is associated with the M6 segment (Zhou et al., 2002; Beck et al.,

2008; Alexander et al., 2009). The relative simplicity, yet similar conductive ability of M2GlyR makes it an optimal platform sequence from which synthetic peptides might be modeled.

The beauty of this approach lies in its direct, yet relatively simple methodology. Unlike palliative options, which merely treat the symptoms of the disease, our peptides have the capacity to restore ion transport across epithelia by delivery (most effectively via aerosolized inhalants) directly into the airways, allowing the peptide to insert in the apical membrane and auto-assemble to form de novo anion selective channels. In addition, as discussed above, unlike gene therapy and similar methods, this method circumvents many of the difficulties in associated with DNA delivery and protein expression.

An optimized channel-forming peptide will exhibit a number of distinct characteristics. Peptides should exhibit solubility in aqueous solution and retain the capacity to form anion conducting channels in epithelial membranes utilizing as little peptide as possible to achieve desired ends. One facet of this faculty requires that the majority of peptide in solution should remain in monomeric form. Peptides that bind cellular membranes in monomeric form have been shown to form functional channels. This factor also contributes to the ability to accurately calculate requisite quantity and concentration of the effectively binding peptide for therapeutic use. Previous studies demonstrated that M2GlyR peptides are generally well-tolerated by mice, eliciting no detectable antigenic effects (Van Ginkel et al., 2008). Because natural electrochemical gradients across cell membranes serve as the driving force for channel permeation, there is little risk of excess secretion.

M2GlyR-altered sequences

Beginning with the M2GlyR sequence, single and multiple amino acid substitutions were explored to improve the properties of the peptide as a potential therapeutic agent. Initial studies with M2GlyR sequences explored both monomeric and tetrameric templated structures following previous general protocols (T₄-M2GlyR) (Mutter et al., 1989; Iwamoto et al., 1994), but the latter was ultimately rejected in favor of the more efficiently synthesized and purified monomer, which showed an increase in short circuit current (I_{sc}) in Manin-Darby canine kidney (MDCK) epithelial monolayers. However, the change in I_{sc} was not immediate and occurred only in a percentage of all monolayers tested. Furthermore, low solubility and uncontrolled orientation of inserted peptide led to the exploration of modified sequences.

In an attempt to better control solubility and insertional orientation, second-generation sequences incorporated terminal oligo-lysine residues. C-terminal pentameric-lysine adducted variants demonstrated the most notable solubility increase, while tetrameric-lysine adducts to either terminus yielded the most optimal balance in solubility and increase in I_{sc} (Tomich et al.,

1998). Furthermore, the C-terminal lysine adducted peptide allowed for the same transmembrane orientation as the corresponding segment in the native glycine receptor, and provided stability in supramolecular assembly of channel formation.

Later studies demonstrated that the modulation of K^+ secretion via Ca^{2+} -dependent channels in the basolateral membrane of epithelia affected the transport elicited by apically-inserted CK₄-M2GlyR in T84 cells. K^+ -channel inhibition by clotrimazole and charybdotoxin resulted in a reduced I_{sc} elicited by the peptide, whereas activators, such as 1-ethyl-2-benzimidazolinone (1-EBIO) amplified the I_{sc} response to equal concentrations of peptide, suggesting coordination between K^+ efflux across the basolateral membrane and fluid as a consequence of Cl^- release. (Wallace et al., 2000). In the presence of 1-EBIO, ion transport by N-terminal lysine-adducted sequences was significantly larger than that of CK₄ peptides at identical concentrations (Broughman et al., 2001; Wallace et al., 1997), and led to the exploration of NK₄-M2GlyR as the lead peptide in the class to develop as a potential therapeutic. Additional studies explored the effect of CK₄-M2GlyR and NK₄-M2GlyR on nasal potential difference (PD) in $\Delta F508$ transgenic mice. Data suggested that pre-exposing murine nasal epithelia to one of the two tetralysine-adducted peptides led to near normalization of Cl^- and fluid secretion relative to CF mice in control groups (in which the expected response was null) and those without treatment (Tomich, Unpublished results).

However, higher I_{sc} at low concentration was not the sole determining factor in selecting a lead sequence and in many regards NK₄-M2GlyR was observed to be suboptimal. Chemical cross-linking, nuclear magnetic resonance (NMR) imaging and computer modeling studies were used to examine the effects of different points of adduction of poly-lysine residues. As hydrophobic residues tend to condense together in solution, aggregation can become problematic with higher peptide concentrations. Ideally, as discussed previously, the majority of the peptide should be monomeric in aqueous solution, without sacrifice of its channel formation and conductance properties. In order to study solution aggregation, bis [sulfosuccinimidyl] suberate (BS3) was used as a cross-linking reagent to lock aggregates into oligomeric form through the use of its free-amine binding molecules. Silver-stained sodium dodecyl sulfate polyacrylamine gel electrophoresis (SDS-PAGE) gels were then used to visualize molecular aggregation in solution (Broughman et al., 2002b). These studies determined that CK₄-M2GlyR sequences exhibit lower aggregation in solution relative to their NK₄ counterparts, with predominant aggregates being those of trimmers and dimers, with much of the peptide remaining monomeric. NK₄-M2GlyR, on the other had, demonstrated considerably greater aggregation, showing oligomers increasing from non-aggregated peptide through 20-mers, as shown in fig. 1.1.

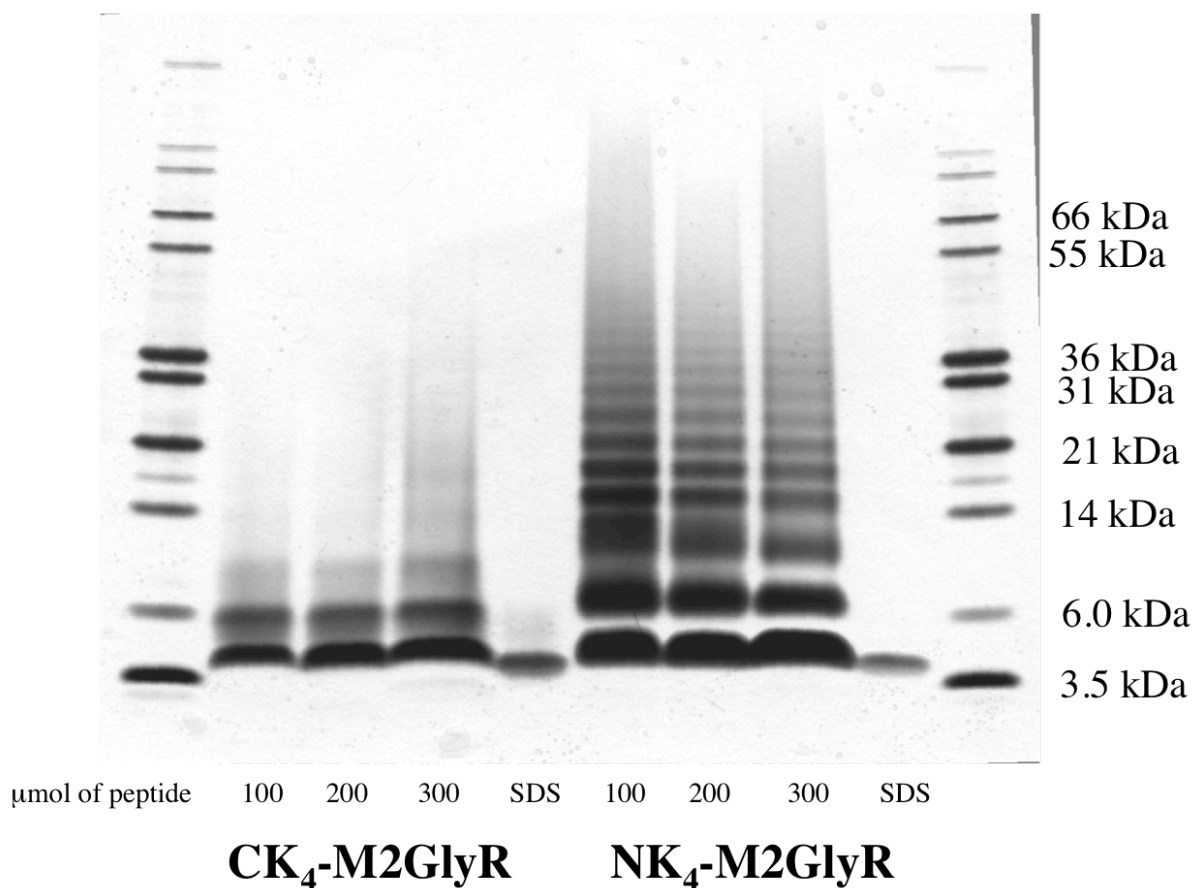


Figure 1.1: Association profile of CK₄- and NK₄-M2GlyR p27

tricine polyacrylamide gel, silver stained, of NK₄-M2GlyR and CK₄-M2GlyR peptides. Lanes 1 and 10 hold standards for molecular weight; lanes 2– 4, NK₄-M2GlyR treated with cross-linking reagent in 40-fold excess (100, 200, and 300 μM, respectively); lane 5, untreated NK₄-M2GlyR boiled in sample buffer containing SDS; lanes 6–8, CK₄- treated with cross-linking reagent in 40-fold excess (100, 200, and 300 μM, respectively); lane 9, untreated CK₄-M2GlyR, boiled in sample buffer containing SDS (reprinted with permission from Broughman et al., copyright 2002b, American Chemical Society).

Further studies sought to determine residues of NK₄-M2GlyR that contributed to aggregation of the peptide in solution. Both NK₄-M2GlyR and CK₄-M2GlyR were truncated at various points and results indicated that truncation of NK₄-M2GlyR’s five C-terminal residues (SGSRA) decreased aqueous peptide aggregation (fig. 1.2) without inducing a notable reduction in I_{sc} (fig. 1.3). In contrast, there was little change in aggregation of CK₄-M2GlyR when residues were truncated from the N-terminal end, but there was a negative effect on ion transport. Ultimately, a truncated form of NK₄-M2GlyR, p22, was adopted as the lead peptide for further study. Furthermore, this shorter peptide was more easily synthesized due to a reduced number of

amino acid additions and therefore more cost-effective to manufacture than any of its counterparts.

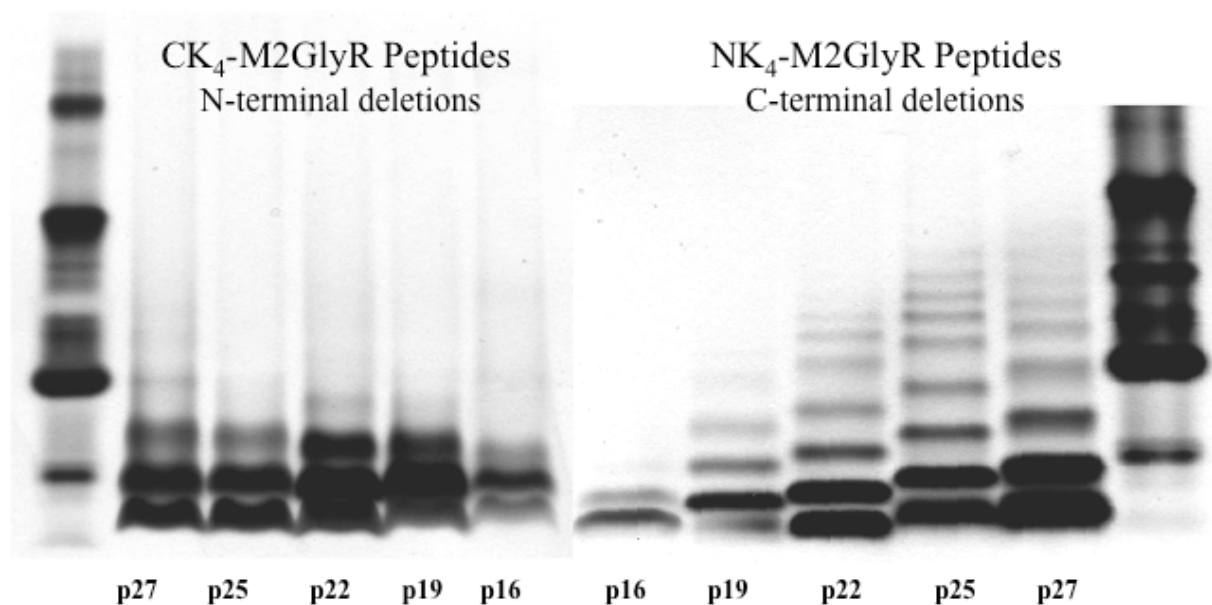


Figure 1.2: Cross-Linked M2GlyR Truncated Peptides

Tricine polyacrylamide gel, visualized with silver stain, of cross-linking patterns for truncated CK₄-M2GlyR and NK₄-M2GlyR. X-axis demonstrates truncation points of the given peptide e.g. p27, truncated at 27 residues, and so on). All samples were treated with a 40-fold excess of crosslinking reagent (Broughman et al., 2002b)

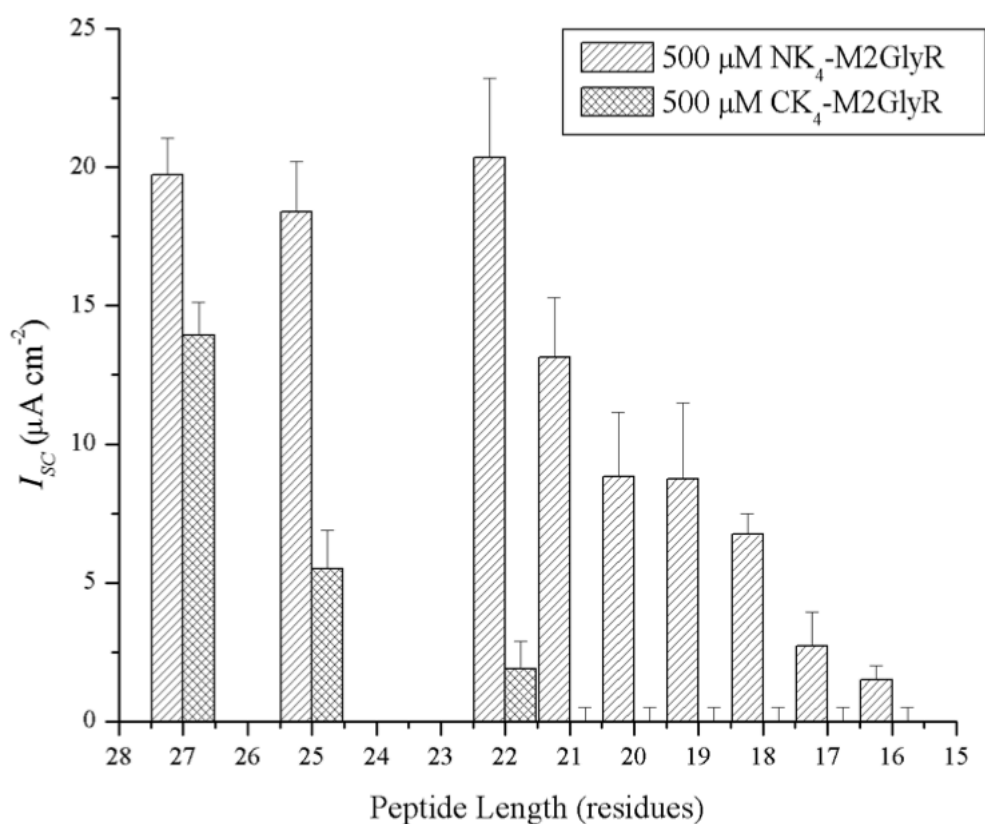


Figure 1.3: Activity of Truncated M2GlyR Segments NK₄- and CK₄-M2GlyR

I_{sc} given by truncated and full-length peptide sequences of NK₄- and CK₄-M2GlyR peptides at 500 μ M in MDCK monolayers. Symbols represent mean and standard error of three to seven observations. (Broughman et al., 2002b)

In eliminating several hydrophilic residues from NK₄-M2GlyR to make its p-22 truncated sequence, the overall hydrophobicity of the peptide was increased, making it less soluble in solution (Wimley and White, 2000; Jayasinghe et al., 2001). This truncation included the elimination of the C-terminal arginine in the truncated NK₄-M2GlyR-p22 sequence, which, as suggested by previous NMR studies on native sequence M2, plays a role in defining the transmembrane domain due to its propensity to lie at the membrane's lipid/water interface (Tang et al., 2002; Yushmanov et al., 2003; Vogt et al., 2000; Harzer and Bechinger, 2000; Mitaku et al., 2002). Subsequent studies were undertaken to explore whether an arginine insertion at the C-terminal end of the truncated NK₄-M2GlyR-p22 might affect solubility, transmembrane positioning and channel conductance (Shank et al., 2006). Results indicated that this arginine substitution at position 19 and beyond dramatically increased aqueous solubility without drastically affecting aggregation patterns or I_{sc} values relative to the parent p22 sequence.

According to several studies, not only arginine, but also tryptophan (Trp; W) has a demonstrated preference to position itself at the lipid/water interface and may therefore play a role in defining transmembrane domains (Braun and von Heijne, 1999; Mall et al., 2004; Demmers et al., 2001; de Planque et al., 2003; Granseth et al., 2005; van der Wel et al., 2007; Hong et al., 2007). A more clearly defined boundary for the transmembrane domain limits peptide mobility within the membrane, restricting its position and reducing deviations in angulation of peptides forming the channel and thereby reducing degrees of freedom. Studies into the substitution of the C-terminal serine of NK₄-M2GlyR-p22 with a Trp demonstrated a notable change in I_{MAX} (maximal short-circuit current observed), $K_{1/2}$ (concentration at $1/2 I_{MAX}$, and Hill coefficient as given by the Hill equation. Though I_{MAX} elicited was reduced somewhat from the parent sequence and similar truncated forms (Broughman et al., 2002b), a significant increase in Hill coefficient and decrease in $K_{1/2}$ suggests that such Trp-substituted peptides are notably more effective than their unsubstituted counterparts at much lower concentrations (fig. 1.4). Cross-linking studies indicated that the S22W form (in which the serine at position 22 is replaced with a Trp residue) was primarily monomeric (Cook et al, 2004). As a bonus, the addition of the 280nm light-absorbing Trp allowed for more accurate concentration determinations via spectrophotometry.

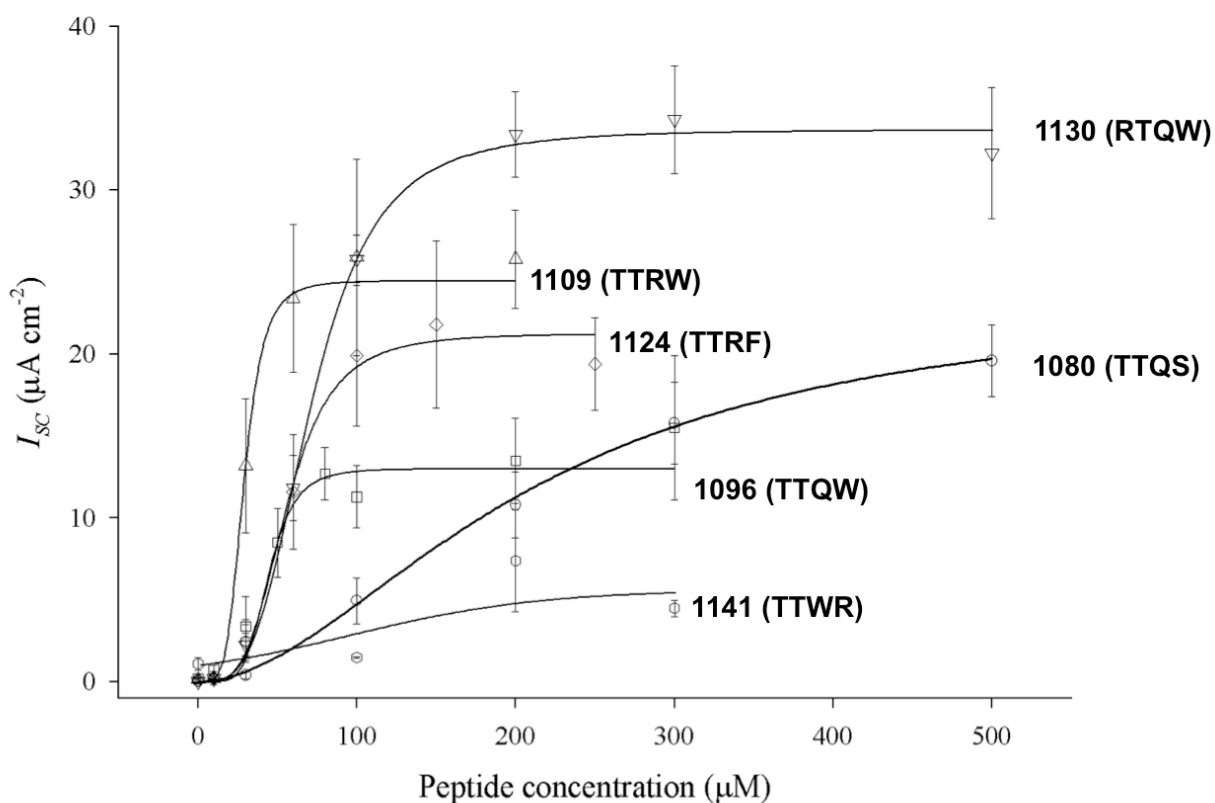


Figure 1.4: Peptide concentration dependence on I_{sc} in MDCK monolayers

Concentration-dependence of I_{sc} by NK₄-M2GlyR-p22 derived peptides with Trp and Arg substitutions on MDCK monolayers. Symbols represent the mean and standard error of 6 or greater observations for each concentration tested. Solid lines represent the best fit of a modified Hill equation to each data set, given by $\Delta I_{sc} = (\Delta I_{MAX} * x^n) / (EC_{50}^n + x^n)$ (further explained in Chapter 2). Letters indicate the final four amino acids for the peptide given by each plot, and is given along with the number code for each given sequence. (Broughman et al., 2002)

The Trp-substituted peptide's ability to resist solution aggregation is an ideal endpoint in the development of a potential therapeutic. As discussed previously, the ability to accurately calculate the concentration of monomeric peptide available for channel formation and utilize as much of the delivered peptide as possible results in lower dosages, minimized excess, and confers economic advantages.

The reintroduction of a positively-charged arginine residue in addition to the tryptophan substitution was hypothesized to affect anion conductance. Further experiments explored the effects of residue substitutions by phenylalanine and tyrosine in place of Trp, and found Trp to remain the optimal aromatic residue for promoting channel assembly. Results indicated that while NK₄-M2GlyR-p22 T19R, S22W and NK₄-M2GlyR-p22 Q21W, S22R demonstrated optimal decreases in $K_{1/2}$, the likely membrane-thinning effects of a C-terminal arginine led its

alternate, NK₄-M2GlyR-p22 T19R, S22W to surface as a lead compound for future study (Cook et al, 2004).

While Trp and Arg-substituted NK₄-M2GlyR p-22 sequences have demonstrated a great deal of promise, relatively reduced aggregation in CK₄-M2GlyR also suggested that the tetra-lys adduct to the C-terminus likely plays a role in countering the nucleation effect of the residues truncated in NK₄-M2GlyR-p22. Despite its apparent advantages in other endpoints, NK₄-M2GlyR is notably less soluble than its CK₄ counterpart in aqueous solution. In an attempt to determine whether CK₄-M2GlyR could elicit similar optimization in kinetic parameters, aggregation, and selectivity when substituted with a pore-defining Trp residue, further study, as presented in the following work, explores whether any of several subsequent Trp-substituted CK₄-M2GlyR sequences might, when explored and modified, warrant further investigation and perhaps demonstrate similar promise as a therapeutic agent for cystic fibrosis.

Chapter 2 - Materials and Methods

Syntheses

NC-1007 (CK₄-M2GlyR) and its related tryptophan-substituted peptides were constructed using N- α -Fmoc protected amino acids (AnaSpec Inc., San Jose, CA) on CLEAR amide resin (0.3 mmol g⁻¹; Peptides International, Louisville, KY) scaled to 0.5 mmol per synthesis. All amino acids were double-coupled. Piperidine (99%) was used for the Fmoc deprotection step, and a solution of 0.225 M for both O-(benzotriazol-1-yl)-N,N,N',N'-tetramethyl-uronium hexafluorophosphate (HBTU) and hydroxybenzotriazole (HOBt) solubilized in dimethylformamide (DMF) was used for the activation step. For capping, 19 ml acetic anhydride, 9 ml N, N-diisopropylethylamine (DIEA), and 6 ml of 1 M HOBt in N-Methyl-2-pyrrolidone (NMP) were combined and further diluted with NMP to 400 ml. Chemicals used were obtained as follows: DMF, NMP, and DIEA from American Bioanalytical, Inc. (Natick, MA), and HBTU and HOBt from Anaspec. Reactions were conducted using 9-fluorenylmethoxycarbonyl (Fmoc) chemistries (Carpino, 1972; Fields, 1990) on a 431A peptide synthesizer (Applied Biosystems, Foster City, CA).

Cleavage, Deprotection and Characterization

The completed peptide bound to resin was suspended in 10 mL of 95% trifluoroacetic acid (TFA) and 5% distilled water and left to set at room temperature for three hours to cleave the peptide from the support and deprotect all side-chain protecting groups (King, 1990). The cleaved peptide was then washed with 30 mL diethyl ether four times, the first of which precipitated the peptide. After being washed with diethyl ether, the precipitated peptide was reconstituted in distilled water, and subsequently extracted by precipitating twice and a final wash with diethyl ether. The peptide was then freeze dried to be used for subsequent experiments. A portion of the dried material was dissolved in 50% trifluoroethanol/water solution and analyzed by Mass Spectrometry using CHCA matrix on a Bruker Ultraflex II MALDI TOF/TOF (Bruker Daltronics, Billerica, MA)

Concentration Determination

For all studies, peptide concentrations were determined spectrophotometrically to a precision of 0.05 μ M using Beer's Law: $A = \epsilon bc$ (where A represents absorbance value as given

by the spectral report, ϵ is molar extinction coefficient of a given residue or residues in $\text{L mol}^{-1} \text{cm}^{-1}$, b represents the path length in cm, and c is the peptide molar concentration). The substituted tryptophan, present in four of the five studied peptides (those altered from the native sequence) provided the chromophore for this application. Because of its aromatic side-chain, a Trp residue absorbs wavelengths in the electromagnetic spectrum at 280 nm, and has a molar absorptivity of 5540 (Edelhoch, 1967; Mach et al., 1992). Absorbance was measured at 280 nm using a Varian Cary WinUV 50 Bio UV spectrophotometer (Palo Alto, CA). Stock samples were diluted by 20-fold for determination, then adjusted to the desired concentrations. In the case of the Trp-free native NC1007, a Bradford Colorimetric Protein Assay kit (Thermo Fisher Scientific, Inc., Rockford, Illinois) was used for concentration determination, the Trp-containing peptide NC1007 G20W was used as a reference for the assay.

Circular Dichroism

In order to evaluate the secondary structure of the peptide NC-1007 (CK₄-M2GlyR) and its Trp-substituted analogs, circular dichroism (CD) studies were undertaken to determine whether the peptide maintained its characteristic alpha-helical structure in both 50% trifluoroethanol (TFE) solution. Prior to characterization, the system was first blanked with 50% TFE solution in which the peptide was to be profiled, absent the peptide itself. This spectra was subtracted from subsequent spectra.

Peptides were first characterized at 100 μM dissolved in 50% TFE in order to record the spectra. TFE acts by stabilizing peptide secondary through the tight association of the TFE molecules with the peptide, displacing water and eliminating the ability of the peptide to form hydrogen bonds with water, thus promoting hydrogen bonding within the peptide, without affecting intra-molecular interaction of nonpolar residues (Roccatano et al., 2002). Spectropolarimeter recordings were performed on a J-720 instrument (Jasco USA; Eaton, MD), and samples were placed in a 1.0 mm cylindrical quartz cuvette. Each recording is a machine-calculated average of five scans per sample. Spectra were assessed from 260 to 190 nm wavelengths at a rate of 20 nm per minute with a 0.2 nm step resolution and 1.0 nm spectral bandwidth and data analysis was performed with software included. Data were recorded in observed ellipticity (θ , in millidegrees, mdeg). However, accounting for peptide concentration, path length, and residue number, mean ellipticity per residue can be calculated using the following equation:

$$[\theta] = (100 * \theta) / ([x]n * l)$$

Where $[\theta]$ is the mean residue ellipticity ($\text{deg cm}^2 \text{decimole}^{-1}$); θ is the observed ellipticity value recorded by the instrument (mdeg); $[x]$, peptide molar concentration; n , total number of amino acid residues comprising the peptide; and l is the path length through the cuvette (cm) (Myers et al., 1997).

Cell Culture

Madin-Darby canine kidney (MDCK) epithelial cells, were originally the generous gift of Dr. Lawrence Sullivan (University of Kansas Medical Center, Kansas City, KS). Cells with passage numbers from 26-41 were cultured on solid substrate culture flasks (T25 Cellstar 25 cm^2 flasks; Frickenhausen, Germany). Culture medium was composed of a 1:1 ratio of Dulbecco's Modified Eagle Medium and Ham's F-12 nutrient mixture (F-12; Invitrogen, Carlsbad, CA), with the addition of 5% heat-inactivated fetal bovine serum (FBS; BioWhittaker, Walkersville, MD), and 1% penicillin/streptomycin mixture (Life Technologies, Invitrogen). FBS contains a number of hormones and nutrients as well as attachment, growth and spreading factors that promote cell growth and proliferation (Gstraunthaler, 2003). The penicillin/streptomycin mixture protects the culture from gram-positive and gram-negative bacterial contamination by disrupting cell wall turnover (penicillin; Doyle et al, 1988), and inhibiting bacterial protein synthesis by binding to bacterial ribosomes, (streptomycin; Cox et al., 1964).

After seeding, MDCK cells were left to proliferate in a 37° C incubator set to contain 5% carbon dioxide. T25 culture flasks that demonstrated 70-90% cellular confluence (roughly four days post-seeding) were subcultured into T25 flasks for further growth or on permeable supports (Snapwell; Costar, Cambridge, MA). Transfer of cells from a given flask was conducted by aspirating medium and rinsing cells with a solution of phosphate-buffered saline (PBS: 137 mM NaCl, 2.7 mM KCl, 10 mM Na_2HPO_4 , 1.8 mM KH_2PO_4). After aspirating the PBS, 0.2 mL of 0.25% trypsin, containing 2.6 mM ethylenediaminetetraacetic acid (EDTA; which acts to break inter-cellular adherence by interrupting the junction of calcium dependent cadherins which form adheren junctions between cells). Remaining solution was immediately aspirated and cells were placed in a 37° C incubator until dissociation was largely complete. Dissociated cells could then be re-seeded into flasks or on permeable supports as mentioned above. Media were refreshed every other day and experiments were conducted within one day of feeding. Permeable supports prepared for Ussing experiments were cultured for a minimum of two weeks (allowed to reach a confluent density of approximately 1×10^6 cells per well) before use.

Transepithelial Electrical Measurements

In order to evaluate the propensity of each given peptide to form pores capable of supporting transcellular ion transport across the epithelial cell membranes, electrical currents were recorded using a modified Ussing chamber (NavicYTE DCV9; San Diego, California) were vertically mounted into vertical diffusion chambers and exposed bilaterally to 10 ml (5 ml each apically and basolaterally) of freshly made Ringer solution (120 mM NaCl, 25 mM NaHCO₃, 3.3 mM KH₂PO₄, 0.8 mM K₂HPO₄, 1.2 MgCl₂, 1.2 mM CaCl₂; Misfeldt, 1976; Hille, 2001). All chemicals used in the production of Ringer solution were acquired from Sigma-Aldrich (St. Louis, MO). Chambers were maintained at physiological temperature (37°) and aerated with a gas mixture of 5% CO₂ and 95% O₂ in order to provide solution mixing in addition to maintaining pH. Each of six MDCK epithelial monolayers, all grown on the same permeable supports as discussed above were measured their initial transepithelial resistance. Monolayers with initial resistance values of less than 200 Ohms cm² were excluded from further testing.

Drugs added during the course of the assay included 1-ethyl-2-benzimidazolinone (1-EBIO; Acros Organics, Morris Plains, New NJ) in dimethyl sulfoxide (DMSO) from Sigma Chemical. Forskolin (*Coleus forskohlii*) was acquired from Calbiochem (La Jolla, CA), and prepared at 10 mM in ethanol.

Transepithelial voltage across the monolayer was clamped at zero using a 558C-model voltage clamp apparatus made by the University of Iowa's Department of Bioengineering (Iowa City, IA), and I_{sc} was recorded continually (Broughman et al., 2001; 2004). Monolayers were exposed to a 5 second 2 mV bipolar pulse between clamped intervals of 90 seconds. Data were acquired at 1 Hz by (Aqknowledge software, version 3.2.6; BIOPAC Systems, Santa Barbara, CA) with an MP100A-CEinterface.

During each experiment, each of the six chambers was allowed to establish stable parameters, and then was exposed to 1-EBIO (100 μ M) to maximize driving force for anion secretion. EBIO hyperpolarizes the epithelia through the activation of Ca²⁺ dependent K⁺ channels in the basolateral cell membrane (Devor, 1996). Although 1-EBIO is capable of stimulating endogenous CFTR, concentrations used in study were significantly lower than those required to increase CFTR channel activity. After establishing a stable baseline I_{sc} , one of five peptide concentrations (30 μ M, 60 μ M, 100 μ M, 200 μ M, and 300 μ M) or a control (300 μ L H₂O) was added apically to each of the six chambers. After recording the changes in I_{sc} for a prescribed period, forskolin (1 μ M) was added to test for cell viability. Forskolin activates adenylate cyclase, an enzyme responsible for the conversion of adenosine triphosphate (ATP) into cyclic adenosine monophosphate (cAMP). Protein kinase A, a phosphorylating agent which

indirectly activates CFTR, increases the secretion of any remaining intracellular Cl⁻ as well as extracellular uptake through the activation of the Na⁺/K⁺/Cl⁻ cotransporter, inducing an observable increase in I_{sc} for intact cells (Carlin et al. 2006; Andrea-Winslow et al., 2001).

Analysis of I_{sc} Data

In order to evaluate the propensity of each peptide to form functional anion-selective channels, ion transport across epithelial cell membrane were analyzed using Microsoft Excel software (Redman, WA). Each data point represents the mean peak change in I_{sc} from baseline (post-EBIO) elicited by each peptide at each concentration from a minimum of five independent observations, where vertical bars represent the standard error of the mean (SEM). Statistical significance was defined relative to a type I error probability of 0.05 or less, as determined via Student's t-test or analysis of variance (ANOVA) assessments in Microsoft Excel.

Lines shown represent the best fit of a modified Hill equation to the data points given:

$$\Delta I_{sc} = (\Delta I_{max} * x^n) / (EC_{50}^n + x^n),$$

In which EC_{50} is the peptide concentration at which 50% of maximal I_{sc} is attained; x is the concentration of peptide; and n is the Hill coefficient. In each case, the fit was constrained and n represents the Hill coefficient. In optimizing the fit to the data sets, I_{max} was constrained to a maximum of the mean value for the maximal peptide concentration observed (300 μ M) + one standard deviation of that data set.

Reverse Phase High Performance Liquid Chromatography (RP-HPLC)

Studies

Lyophilized stock peptide was dissolved in 100 μ l trifluoroethanol and diluted with 100 μ l of ultrapure deionized water for a final concentration of approximately 3 mg/ml in a solution of 50% TFE. The peptide was assessed by HPLC (System Gold HPLC; Beckman Instruments, Fullerton, CA) using a reverse-phase C-18 column (Phenomenex, Torrance, CA). Two solvents were gradated with one another to elute peptide from the column: Solvent A, composed of 0.1% trifluoroacetic acid (TFA) in ultrapure deionized water, and solvent B, consisting of 0.1% TFA in 90% acetonitrile, 10% water. Successive gradation, sustention, and re-equilibration characterize the course of the HPLC profile. Free salts elute first from the system with peptides remaining bound to the column's solid phase during the five-minute stable flow of 10% Solvent

B and 90% Solvent A. Next, the peptide was eluted during the course of a linearly increasing 30-minute graduation of the ratio of solvent B (TFA in ultrapure water) to solvent A (acetonitrile) from 10:90 to 90:10 during which peptides are generally released with the mobile phase near the 20-minute mark. After the gradient stage, the end ratio of 90:10 solvent B: solvent A was maintained for five minutes to elute any remaining substances in the column. Elution was monitored by the UV detector at 220 nm

UV/Vis Spectrometry

Absorbance spectra were employed to determine whether the peptide demonstrated a patterned violet shift characteristic of tryptophan (standard absorbance, 280 nm) protected within the hydrophobic environment of the aggregate for peptides (one each in which the substituted tryptophan was located within the hydrophobic or hydrophilic faces of the helix as determined by helix wheel modeling described in the next chapter) as compared to that of the free amino acid from Sigma-Aldrich. Samples of NC1007 S18W and NC1007 G20W (selected for the clearly defined location of the ω -substitution in the hydrophobic and hydrophilic regions, respectively), as well as free tryptophan were prepared (5 mM in water) and profiled from 200 to 400 nm at a rate of 300 nm/min using a Varian Cary WinUV 50 Bio Ultraviolet/Visible spectrophotometer (Palo Alto, CA).

Chapter 4 - Results and Discussion

Characterization

The purpose of the following studies was to assess whether alterations to the CK₄-M2GlyR peptide sequence, initially modeled after the second transmembrane segment of the spinal cord glycine receptor, via the sequential substitution of a Trp residue for C-terminal residues would affect secondary structure, solution aggregation, channel formation, and ion permselectivity.

The peptides are denoted as derivatives of the NC-1007 sequence. The control and modified sequences, with the substituted Trp in bold typeface are shown in **Table 4.1** along with molecular weights. These positions were selected with the hypothesis that the added Trp would serve as the interfacial residue for the C-terminal portion of the peptide. Previous work showed that Trp substitutions in N-K4-M2GlyR eliminated solution aggregation (Broughman et al., 2002). Thus we anticipate a similar effect for one or more of the peptides prepared in this study.

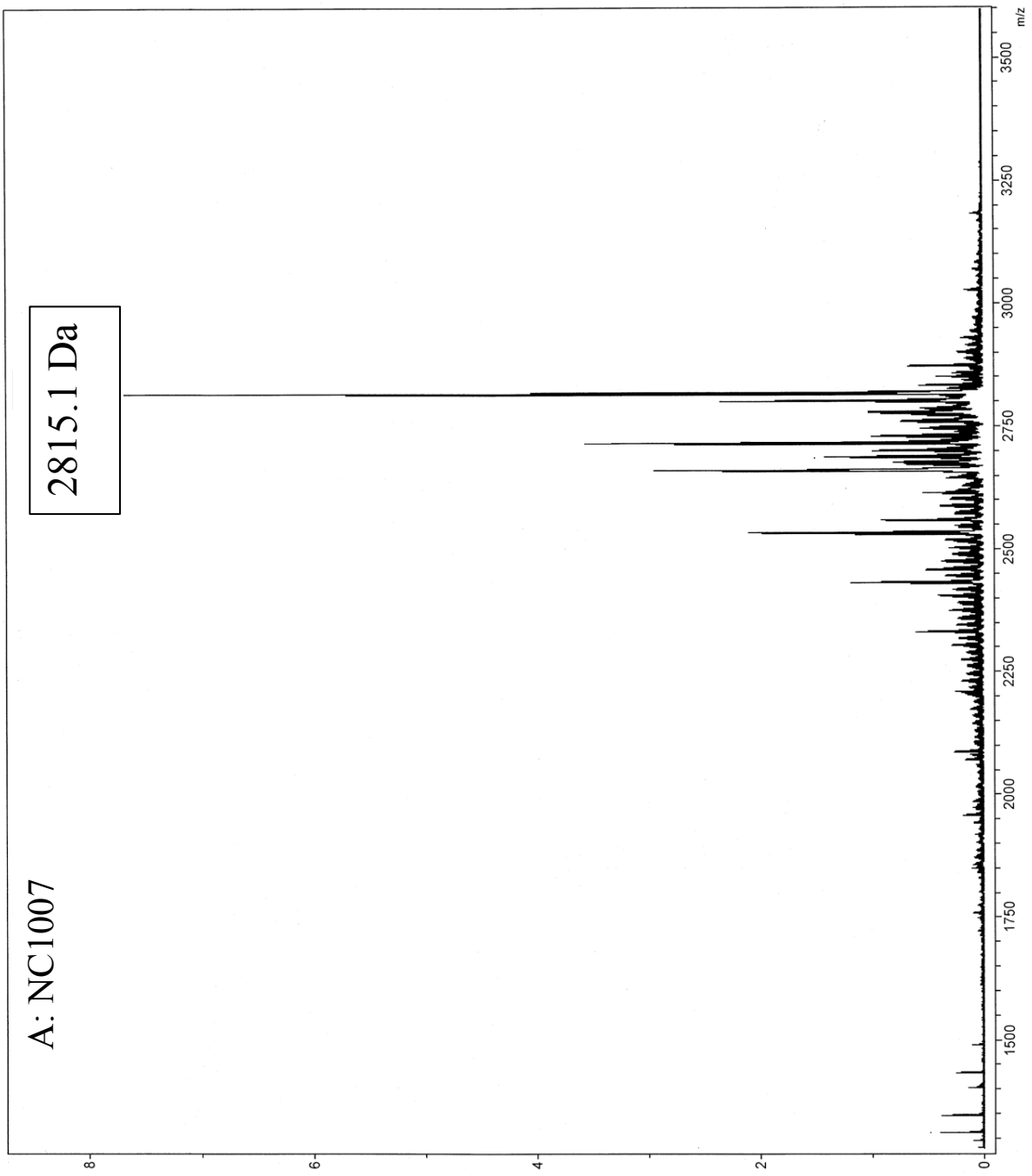
Peptide	Conventional Name	Sequence	Molecular Mass (Da)
CK ₄ -M2GlyR-	NC-1007	PARVGLGITTVLTM T TQSSGSRAK K K K K	2815.6
CK ₄ -M2GlyR-S18W	NC1007 S18W	PARVGLGITTVLTM T TQ W SGSRAK K K K K	2914.6
CK ₄ -M2GlyR-S19W	NC1007 S19-W	PARVGLGITTVLTM T TQ S WGSRAK K K K K	2914.6
CK ₄ -M2GlyR-G20W	NC-1007 G20W	PARVGLGITTVLTM T TQSS W SRAK K K K K	2944.6
CK ₄ -M2GlyR-S21W	NC1007 S21W	PARVGLGITTVLTM T TQSSG W RAK K K K K	2914.6

Table 4.1 Conventional name, sequence, and molecular mass of experimental w-substituted variants of NC1007

The sequence in which the C-terminal serine21 was substituted with Trp posed the most abnormal behavior in several aspects, and had to be synthesized multiple times to obtain an effective batch of the proper sequence. Arginine-containing sequences are often pose difficulties

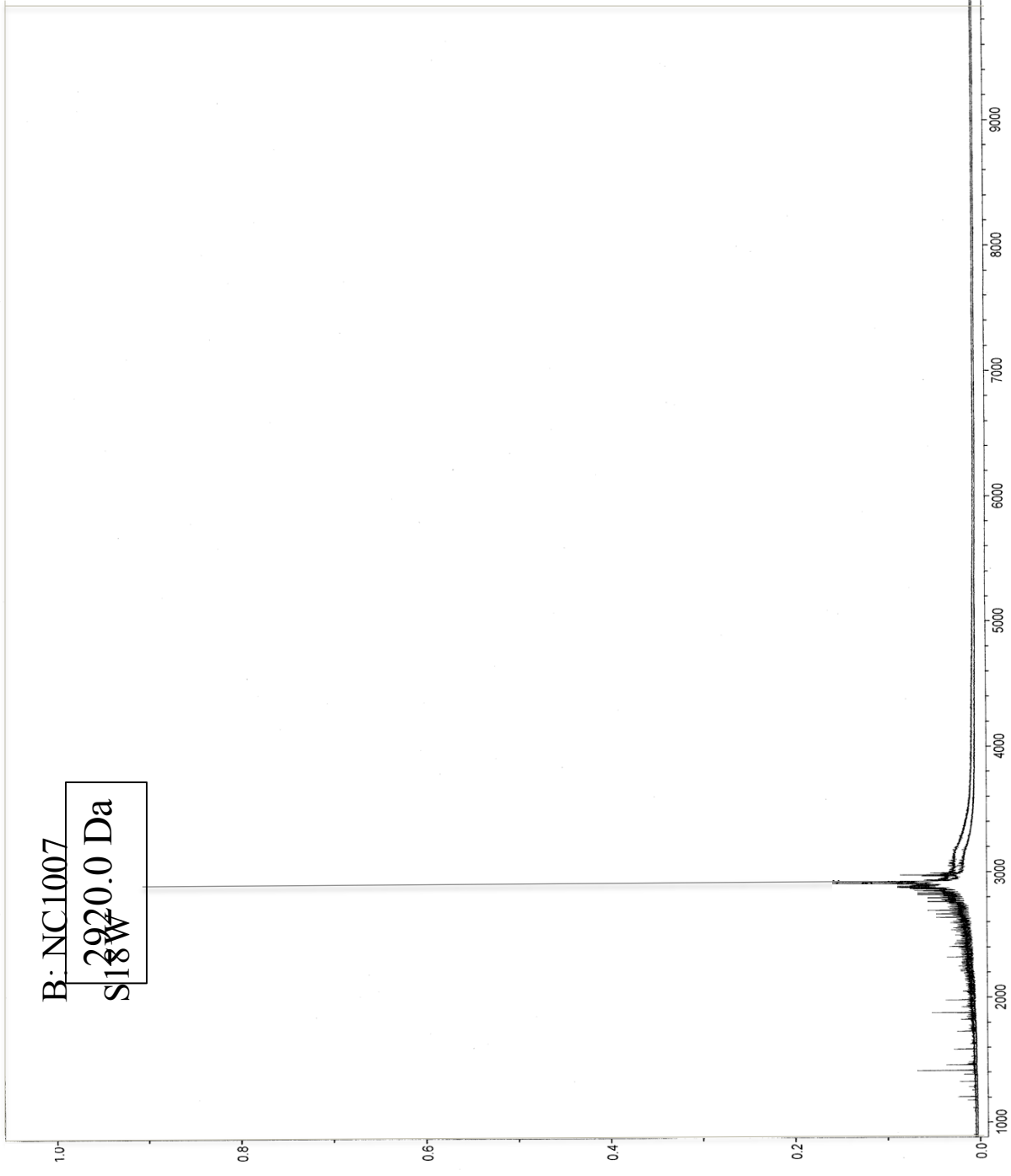
in synthesis due to poor coupling efficiencies of bulky amino acids that are added immediately after the arginine. This is true in the case of the S21W sequence. It is important to note that peptide synthesis occurs in the C- to N- direction so in the case of S21W the tryptophan is added after the arginine.

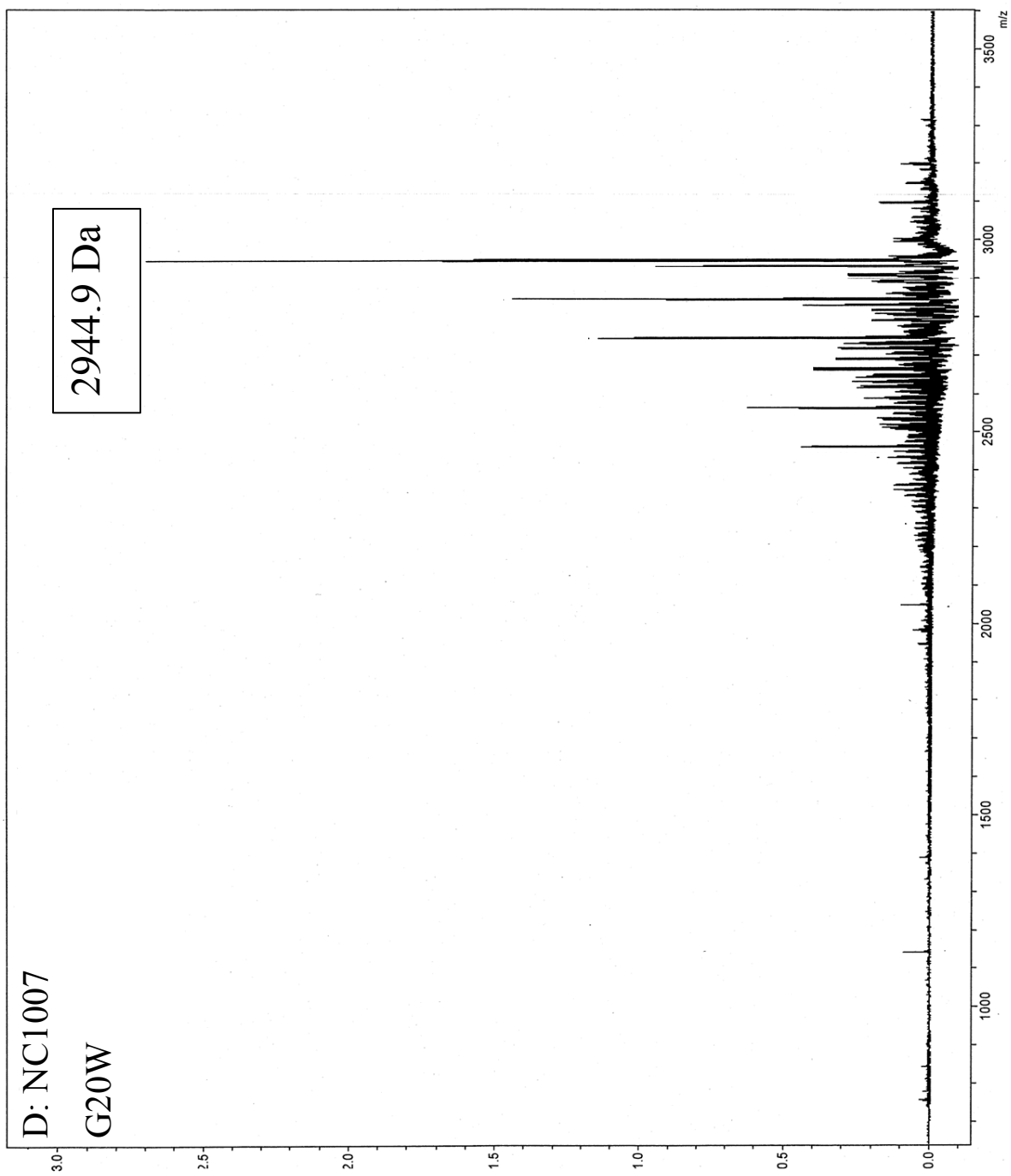
After synthesis, peptides were characterized by MALDI-TOF spectrometry. Results are shown in **Fig. 4.1**. In all of the MS tracing the desired product is observed for all of the syntheses as well as a number of other peaks generally of lower mass. Due to differences in moving the different components of the synthetic mixture into the gas phase this method is not quantifiable. Peak heights bear no relationship to relative concentrations, and unlabeled peaks are remnants of failed sequences, commonly those with amino acid deletions.



C: NC1007

S19W





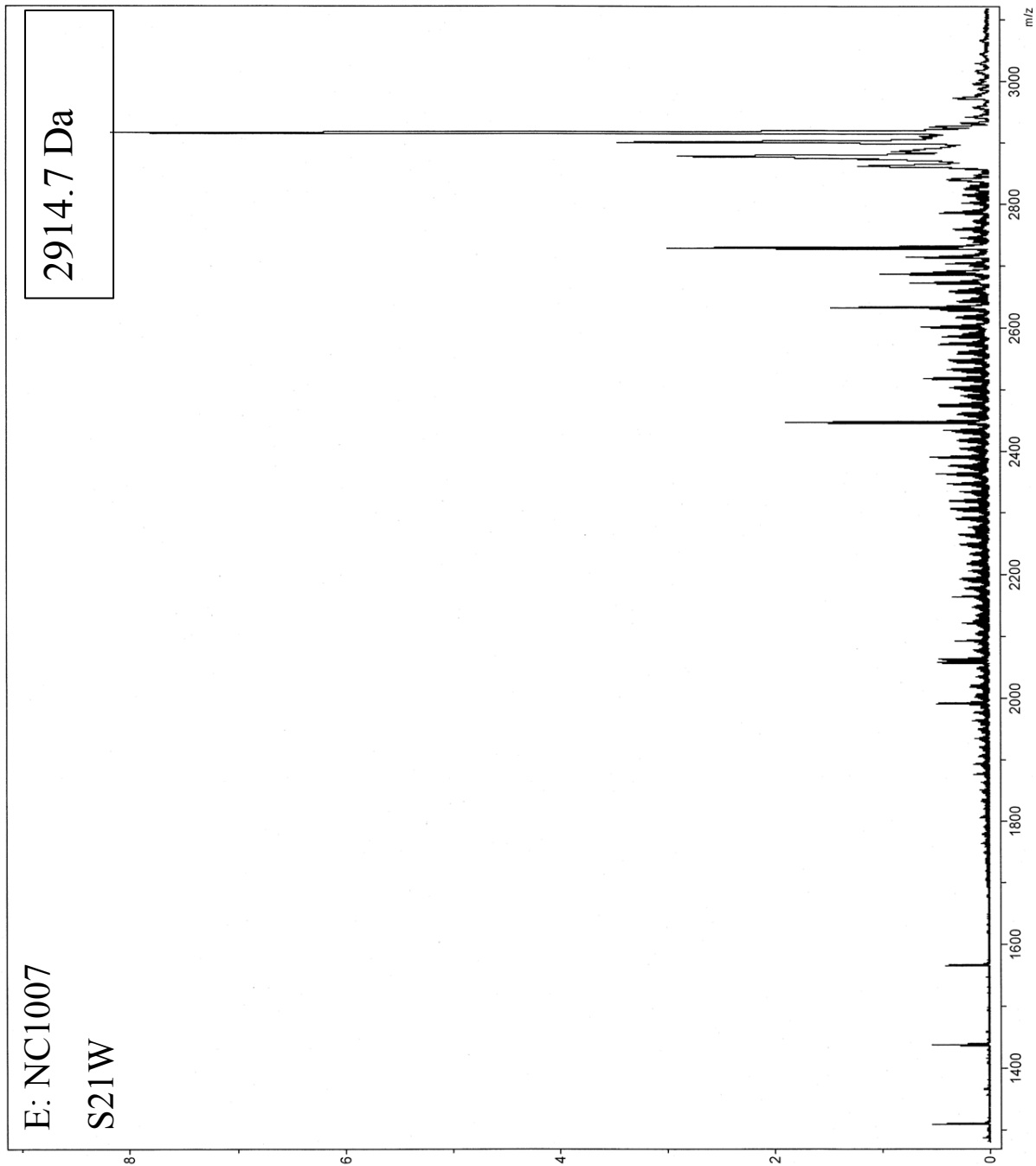


Figure 4.1 (A-E) MALDI-TOF spectral profiles for experimental peptides

A: NC-1007, MW 2815.1 Da; B: NC-1007 S18W, MW 2917.2 Da; C: NC-1007 S19W, MW 2920.0 Da; D: NC-1007 G20W, MW 2944.9 Da; E: NC-1007 S21W, MW 2914.7 Da

X-axis indicates mass/charge ratio, and Y-axis indicates intensity, in arbitrary units ($\times 10^4$).

Circular Dichroism

Circular dichroism (CD) studies were undertaken to determine whether the Trp-substituted peptides maintained characteristic alpha-helical structure both in solution. After determination of effective synthesis by MALDI-TOF spectrometry, peptides were reconstituted

at 100 μM in 50% TFE for the CD structural determination experiments. All peptides, including NC-1007 S21W adopted α -helical conformations both in micelles and in solution as judged by the presence of characteristic minima at approximately 222 and 208 nm. TFE acts to stabilize secondary structure by hydrophobic interaction, preventing the peptide from forming inter-peptidyl hydrogen bonds, and promoting intra-peptide bonding. Shown in **Fig. 4.2.** are data presented in mean molar residue ellipticity versus wavelength. From these results it is apparent that the introduction of the Trp residues does not affect the ability of the peptides to adopt a characteristic helical structure in membrane-like environments. Previous studies have suggested that peptides that fail to form helical structures in TFE also were ineffective at stimulating I_{sc} . (Broughman, 2002)

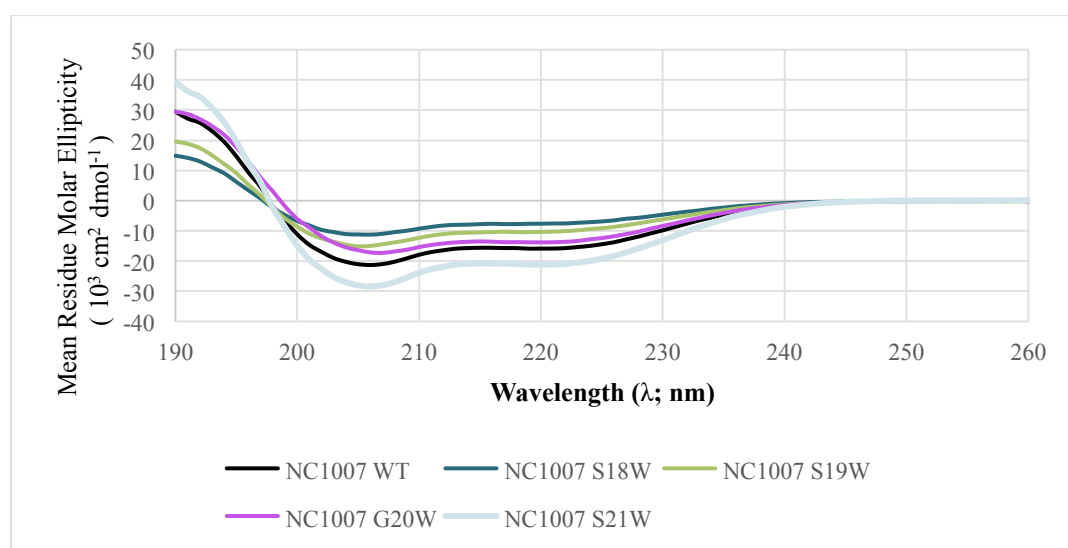


Figure 4.2: Circular Dichroism profiles of NC1007 W-substituted peptides

Spectral profiles indicate characteristic α -helical structure with local minima at around 208 and 220 nm at 100 μM in 50%TFE

Measurements of I_{SC} were used to determine the concentration-dependent effects of Trp-substituted NC-1007 sequences on ion transport. After establishing a consistent baseline, cells were exposed to 1-EBIO, and allowed to achieve a new stable baseline. I_{SC} was recorded for the EBIO treated monolayers immediately prior to peptide exposure. 1-EBIO works by stimulating potassium (K^+) channels in the basolateral membrane. The resultant movement of this positively charged ion acts to further hyperpolarize the cell, stimulating increased flux of Cl^- by amplifying electrochemical driving force for anion secretion, and therefore, the measured response (Devor, 1996; Broughman et al., 2001).

In each at least five independent trials per concentration (30 μ M, 60 μ M, 100 μ M, 200 μ M, and 300 μ M) per peptide, NC-1007 and its tryptophan containing variants were added to the bathing solution of the apical portion of the chamber. Immediately upon peptide addition, a response in I_{SC} was clearly noticeable at the higher concentrations, uniformly peaking within the first two to three minutes after exposure, and in some cases eliciting currents greater than 25-30 μ A. In these cases after reaching the peak current a gradual decline in I_{SC} was seen, most likely due to a partial polarization of the cells, conditions that would reduce the driving force for chloride efflux. After a minimum of 10 minutes of recording the peptide induced I_{SC} , forskolin (2 μ M) was added both apically and basolaterally to the chamber to test for post-treatment viability and membrane integrity. The course of additions in a typical Ussing run is shown in **Fig 4.3**.

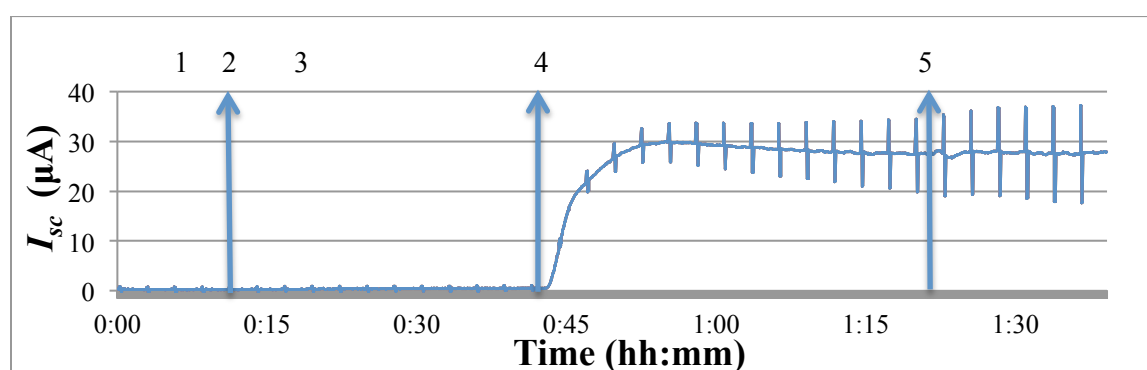


Figure 4.3 Course of a typical Ussing chamber experiment

- 1) post-mount equilibration
- 2) addition of 100 μ M 1-EBIO
- 3) establishment of baseline current
- 4) addition of peptide
- 5) addition of 2 μ M Forskolin

MDCK monolayers exhibited a concentration-dependent increase in I_{SC} in response to the addition of all of the peptides. Maximal current values as averaged over 90 second clamped increments between pulses were collected for each concentration in each trial (one trial

consisting of one peptide tested at five concentrations), and cumulatively used to determine the best fit in the modified Hill equation after subtraction of post-EBIO baseline values.

Generally, as shown in the plots of peptide concentration relative to ΔI_{SC} (**Fig. 4.4**), complete saturation was not reached using the concentrations tested. In all cases except in that of NC1007 S21W, constraining the I_{MAX} value to the mean I_{SC} value at 300 μM + one standard deviation produced the best fit of a Hill equation to the data. The I_{SC} value of constrained fits as well as values for $K_{1/2}$, and the Hill coefficient (n) were determined by the best fit of the modified Hill equation given in Chapter 3, as obtained using SigmaPlot (Systat Software, San Jose, CA) and presented with their respective standard error of the mean (SEM) in **Table 4.2**.

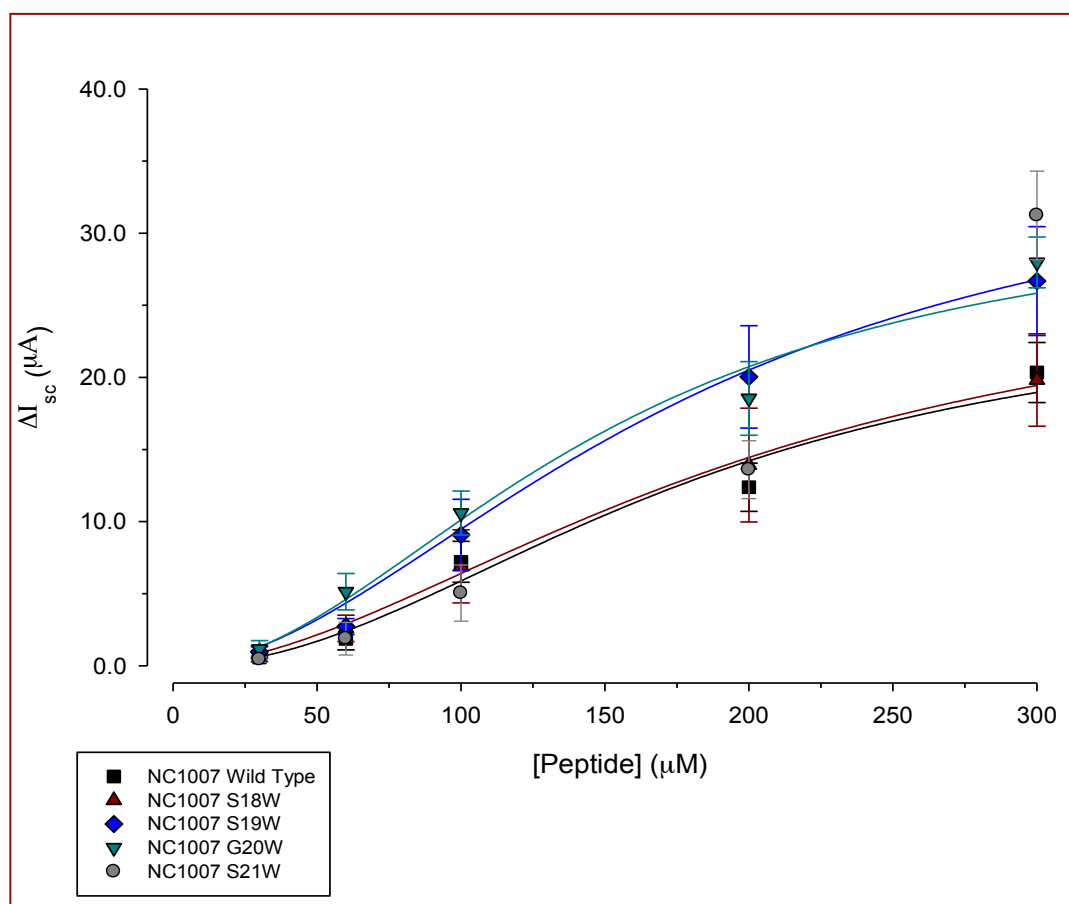


Figure 4.4: Concentration-dependence of peptide on peak ΔI_{sc} across MDCK epithelial cells
 Symbols represent the mean, and error bars represent \pm SEM for a minimum of four observation per data point. Solid lines represent the best fit of a modified Hill equation to the data. Note that though data points are presented, there is no demonstrated fit of the mathematical model given to the data derived from NC-1007 S21W.

Table 4.2 Kinetic Parameters of W-Substituted NC1007 Peptides

* I_{MAX} values were constrained to less than or equal to the mean value at the highest concentration tested for each peptide (300 μM in all cases) + 1 standard deviation. It is assumed for the sake of the experiments conducted that I_{MAX} approximates ΔI_{SC} values observed at the highest tested concentration.

**Kinetic parameter data not available for NC-1007 S21W

Peptide	I_{MAX} (μA)*	$K_{1/2}$ (μM)	Hill coefficient (n)
NC-1007 WT	25.4 \pm 9.4	178 \pm 79	2.07 \pm 0.77
NC-1007 S18W	28.2 \pm 21.6	195 \pm 187	1.84 \pm 1.15
NC-1007 S19W	36.7 \pm 17.9	176 \pm 111	1.86 \pm 0.87
NC-1007 G20W	32.3 \pm 8.2	149 \pm 50	1.98 \pm 0.62
NC-1007 S21W	n/d**	n/d**	n/d**

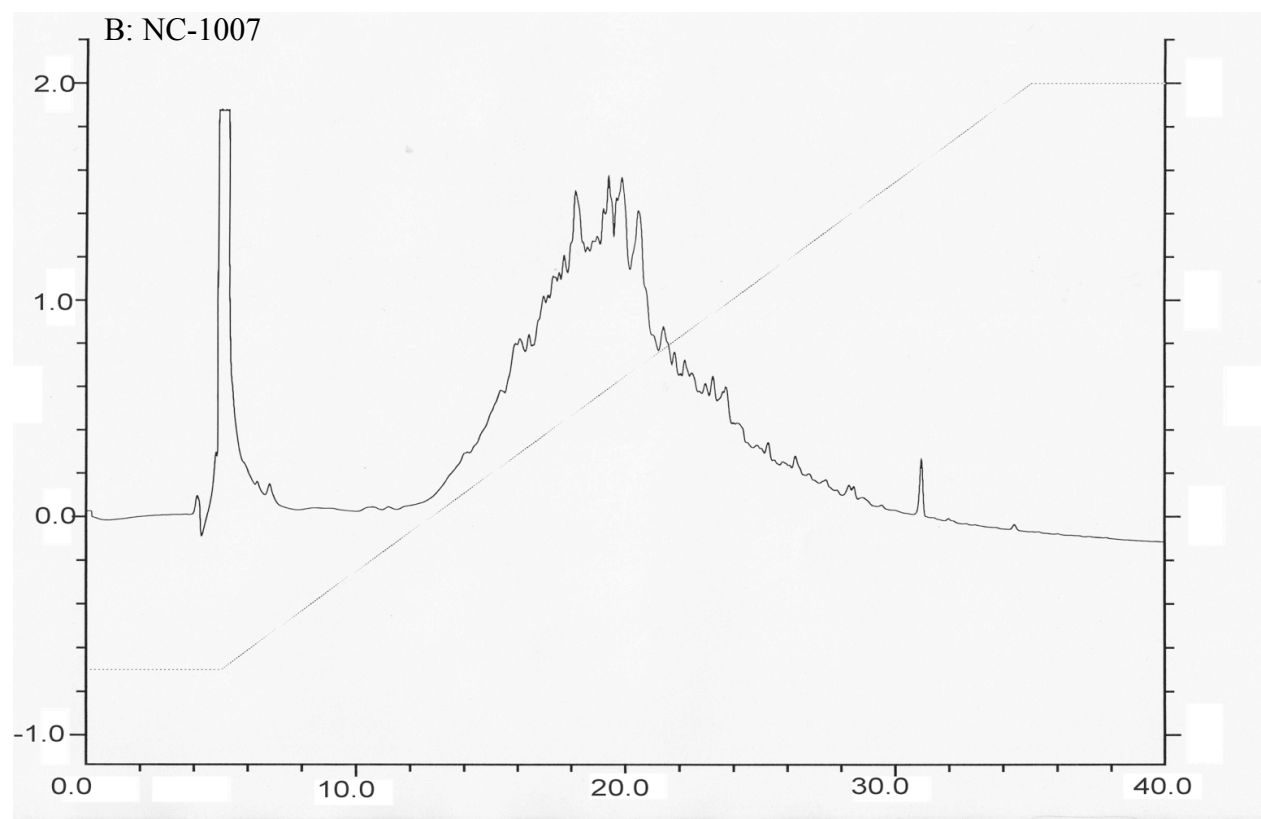
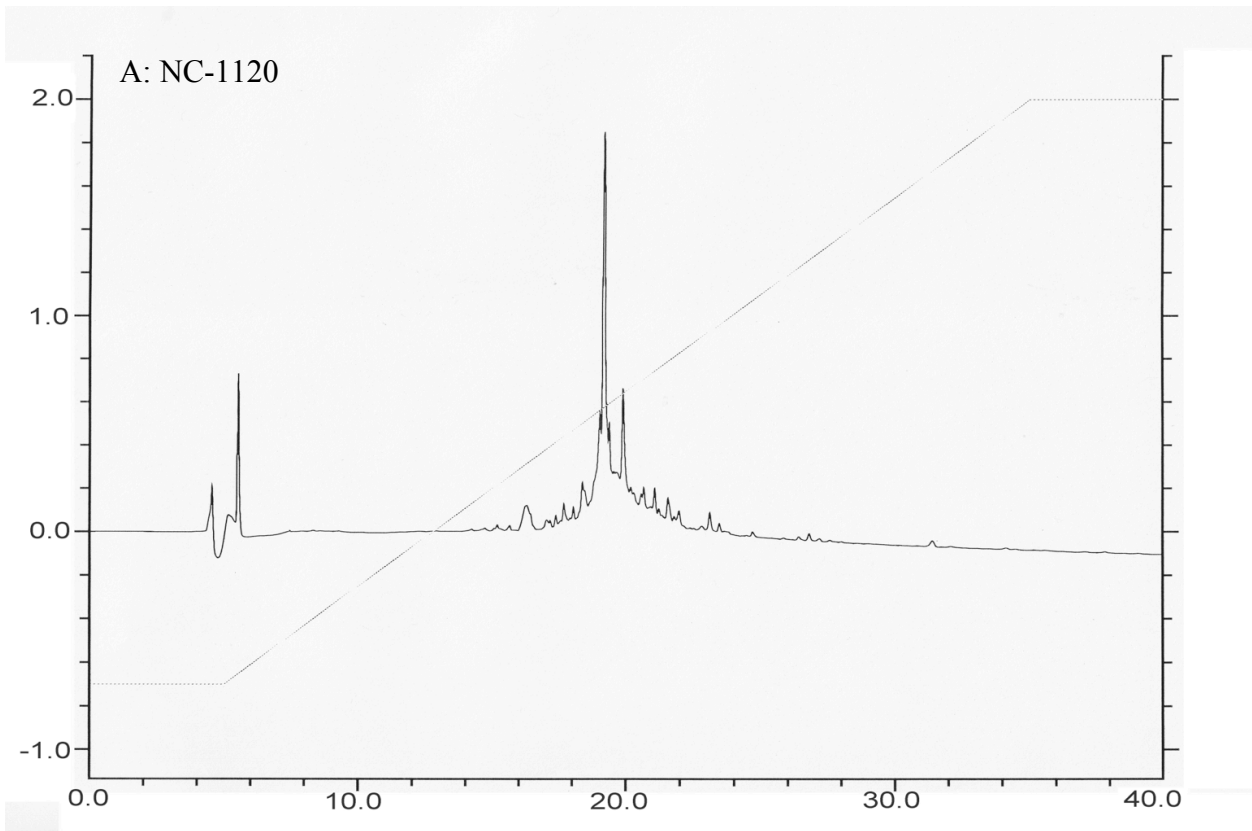
Despite multiple attempts, NC-1007 S21W data could not reasonably be fit by the Hill equation presented. Attempted fits using SigmaPlot software yielded results with kinetic parameters vastly different than any related sequences. All modified peptides appeared to be best fit with a higher I_{MAX} value than their unmodified counterpart. Interestingly, while unconstrained $K_{1/2}$ and Hill values given in **Table 4.2** remain roughly in the same range for all peptides excepting NC-1007 S21W (ranging from around 150 to 200 μM and 1.84 to 2.1, respectively), there appears to be uniquely consistent patterns in some cases. Substituting a Trp for serine at

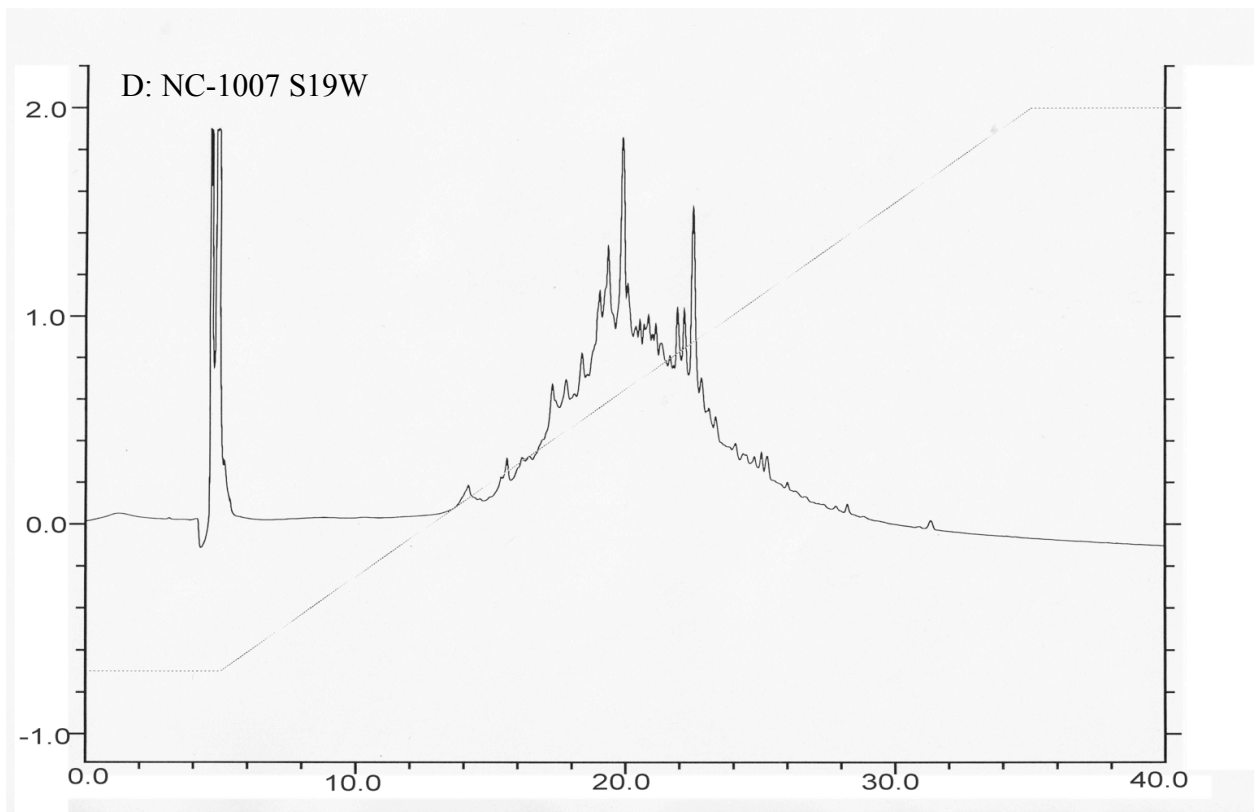
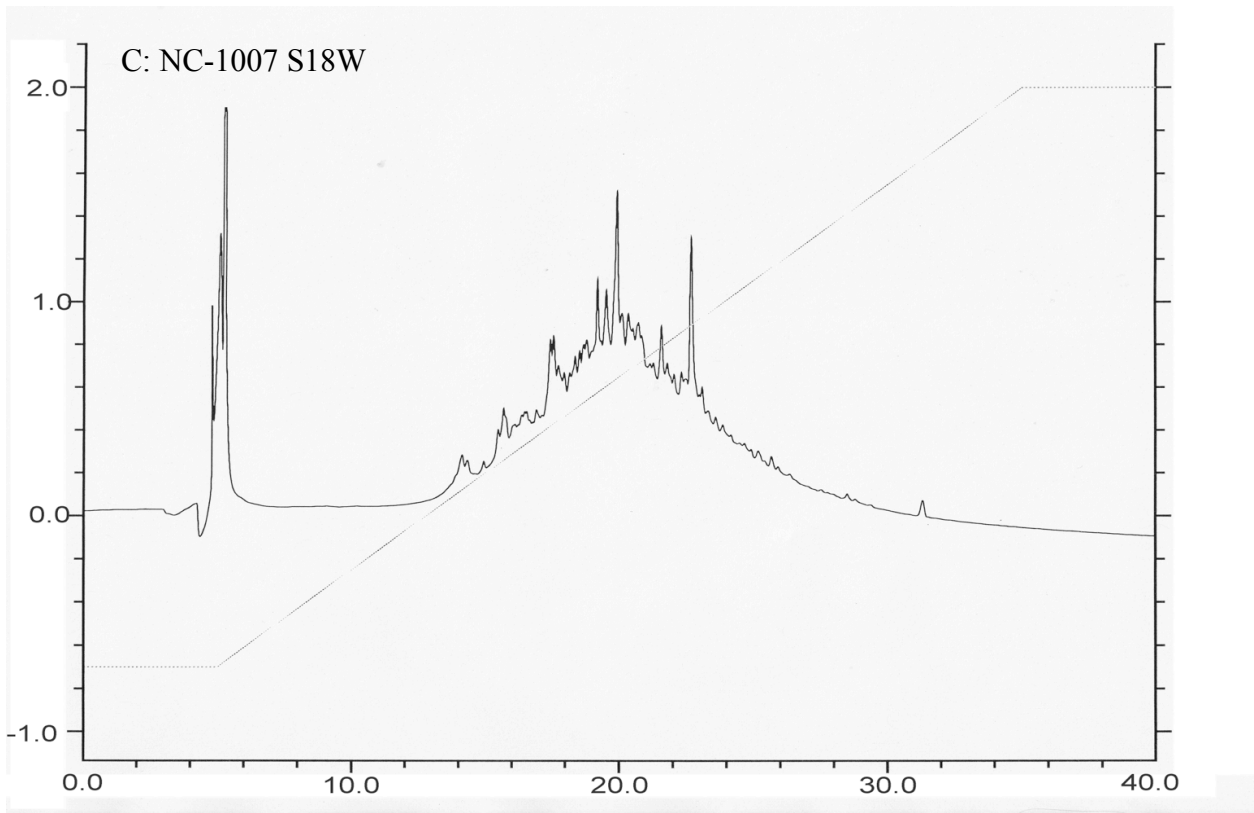
position 18 in the sequence, while slightly increasing $K_{1/2}$ and decreasing the Hill coefficient, produced an overlay to the line of fit rendered for the data of the native sequence peptide, suggesting that this slight decrease in Hill and increase in $K_{1/2}$ have a net effect of a very similar concentration-dependence curve as shown in **Fig. 4.4** below. Similarly, a tryptophan substitution in either the 19th or the 20th position in the peptide sequence (for serine and glycine, respectively), produced a similar net effect in either case, though clearly distinct from those of the unmodified sequence or NC-1007 S18W.

Though the Hill coefficient is generally assumed to be an indicator of cooperativity in channel formation, the data presented with Hill coefficients in all cases exceeding a value of one are alone insufficient to characterize channel formation, but do reflect that the channel structuring process is more complicated than a simple bimolecular interaction.

RP-HPLC Studies

Peptide samples were analyzed by HPLC. Monomers elute as sharp peaks while aggregates elute as broad poorly defined humps. **Fig. 4.5** shows the chromatographic profiles of all peptides tested, including that of a previously studied peptide, NC-1120, known to be in a predominately monomeric form (Broughman, 2002). Previous studies showed that CK₄-M2GlyR (NC-1007) adopted multiple assemblies in water. The three major species observed were monomer, dimer and some higher form, perhaps tetramer. We hypothesized that the substitution of a Trp near the C-terminus may reduce the aggregation propensity of the carboxy-terminal lysyl-adducted peptides. Results indicate, however, that this substitution had little effect on the maintenance of a monomeric solute, and subsequent reanalysis of various obtained fractions along the HPLC profile simply produces an identical chromatograph to the sample from which such fractions were initially obtained. These results suggest that aggregate dominates all tested variants of NC-1007 in solution, as no amount of collection and reanalysis of peptide sample was capable of reducing the profile to a well-defined peak such as that demonstrated in the comparison sequence, NC-1120 (Broughman et al., 2002).





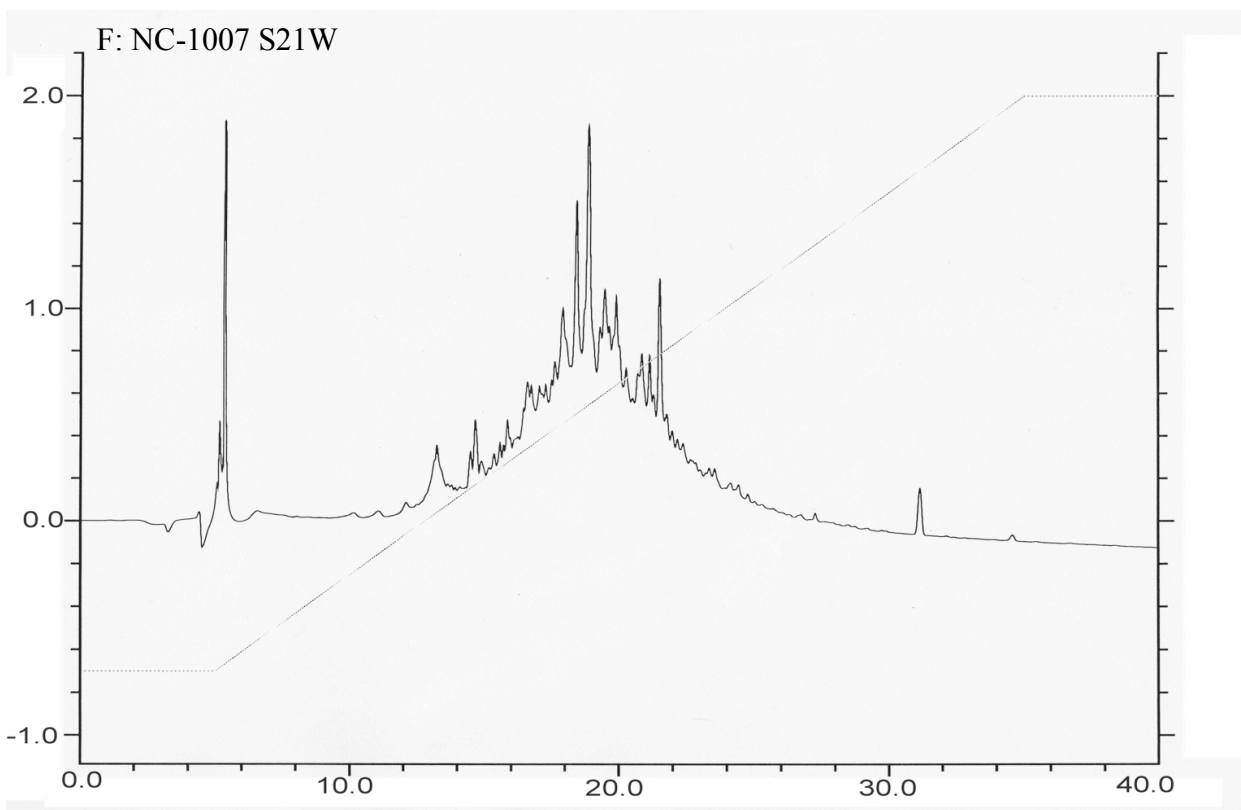
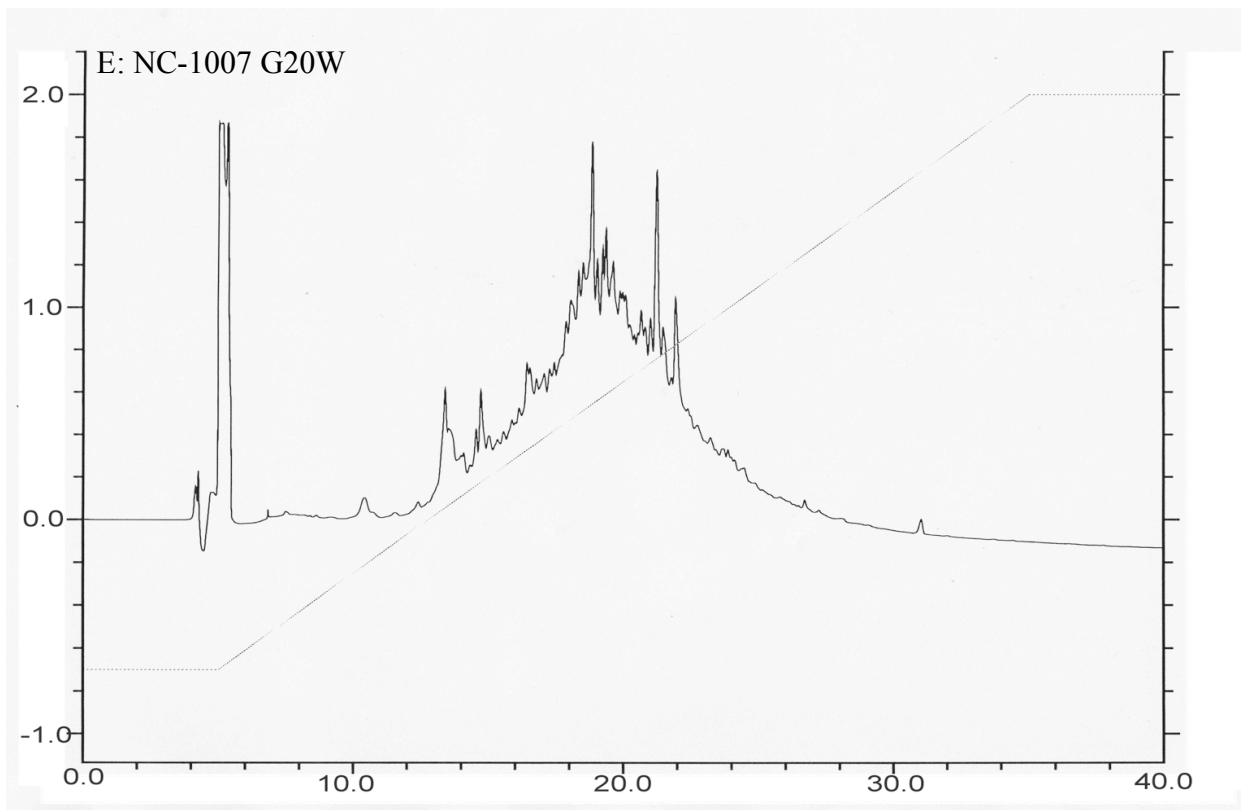


Figure 4.5 (A-F): HPLC chromatographs of Trp-substituted peptides

All experimental peptides demonstrate aggregation relative to a known monomeric sequence (A: NC-1120), and the unmodified sequence, known to form solution aggregates (B: NC-1007).

Discussion

The aim of these studies was to explore whether tryptophan residue substitutions in the C-terminal region of NC-1007 (CK₄-M2GlyR; PARVGLGITTVLTM₁TTQSSGSRAK₄KKK) would ameliorate solution aggregation while optimizing positioning of the transmembrane portion of the sequence such as to induce desirable changes in kinetic parameters of ion flux (e.g., increase in I_{MAX} , reduced $K_{1/2}$). Such an approach was employed successfully on peptides containing the N-terminally adducted lysines. Peptides such as NC-1130 (NK₄-M2GlyR T19R,

S22W; KKKKPARVGLGITTVLTMRTQW) showed little solution aggregation and showed an increased I_{MAX} and a reduced $K_{1/2}$ relative to the native sequence. Unfortunately this sequence was no longer anion selective. NC-1007 is anion selective and by incorporating these substitutions in the region known to promote aggregation we hypothesized that aggregation could be reduced without reducing selectivity.

The Trp-substituted variants of the peptides analyzed in this study, produced mixed effects with regard to their electrophysiological properties. One unexpected outcome demonstrated by electrophysiological studies, is the approximate overlap of data fit to a modified Hill plot between peptide pairs. The S18W substitution gave results similar to the unmodified sequence. The S19W and G20W sequences produced slightly higher currents but their concentration for half-maximal currents were unchanged over the unmodified NC-1007. The S21W variant gave atypical results in that at lower concentrations it behaved more like NC-1007 but at the highest concentration it produced currents even higher than any of the other sequences. These complementary profiles suggest an interesting correlation between concentration-dependent effects on ion flux and placement of tryptophan in the peptide sequence. As discussed previously, a typical membrane-spanning helical domain is composed of about 18-20 amino acid residues. However, the membrane can “thin” such that as few as 14 residues may span the membrane in helical structure (Hille, 2001). Though Arg has been noted to play a role in defining the barrier of the transmembrane segment, hydrophobic Trp has also been shown to be important in defining pore registry within the membrane. It is possible that the similar kinetic profile of S18W to that of the wild type may be explained by the propensity of the peptide to span the membrane from Arg to Arg (18 intermediate residues), rather than sufficiently driving the membrane to “thin” to its minimal capacity in order to contain merely the 14 residues between the registry-defining N-terminal Arg and the Trp in the 18th position in the sequence. Setting aside any assumptions about how the bulky aromatic Trp residue might affect the channel structure and kinetics, this identification in registry could explain the similar overlay of NC1007 S18W to that of NC1007.

It is also conceivable that an elongating shift in tryptophan position from the 18th to the 19th or 20th sequential position might allow for a more energetically favorable conformer in which the tryptophan was sufficiently distant from the N-terminal arginine to define the span as hypothesized. Such a schema may explain the similarity in profile between NC1007 S19W and NC1007 G20W (a single amino acid shift). Notably, however, NC1007 S21W behaved like none of its Trp-substituted counterparts, defying the mathematical model used to describe all other experimental peptides studied, suggesting a more complicated interaction than that described by the model. The proclivity of both Arg and Trp to lie at the membrane interface could perhaps

shed light on one facet of this notable difference. Notably, NC1007 S21W is the only peptide studied in which the C-terminal Arg and substituted Trp are adjacent to one another. It may be problematic in that neither of the two residues clearly and consistently defines the registry in this sequence, leading to inconsistency not only in the membrane placement of each peptide forming the channel, but also the position of a single peptide (or channel) over time.

Trp-substituted variants had no measurable effect on solution aggregation. Solution aggregation prevents HPLC purification of the desired product since any purified and dried material upon redissolving in water regenerates the aggregated state and produces a replicate profile identical to the initial profile. The similarity in profile upon repeat runs suggests not only that the peptide is likely to continue aggregating after fractionation, but also that there appears to be no concentration-dependent change in the relative amount of aggregate peptide in solution.

To further characterize the aggregate form of the peptides, the UV absorbance properties of the Trp-containing sequences were analyzed. The free Trp control, which is completely solvent accessible, gives a sharp absorbance peak centered around 278-280 nm. In contrast all of the peptides show much broader peaks with the added absorbance extending into the lower wavelengths, suggest of a blue shift for some of the tryptophan residues. One could conceivably image two peaks merging to give the resultant peak. Since there are no other chromophores in the peptides, this result indicates that the Trps are present both in solvent exposed and buried environments. All of the profiles look similar suggesting that the location of the added tryptophan relative to the hydrophobic and hydrophilic faces of the helices has no bearing on their solvent accessibility in the aggregate state.

To examine potential positional effects of the tryptophan substitutions in the amphiphilic helix, the sequences were examined visually with regard to their location in the hydrophobic face, or the hydrophilic face that would exist when the helices self-assemble to form the channel pore. Under these conditions, helix wheel representations of NC-1007 and Trp-substituted variants were modeled using Emboss Pepwheel software from Alan Bleasby (European Bioinformatics Institute, Hinxton, Cambridge, United Kingdom; Rice et al., 2000), omitting the C-terminal tetra-lysyl tail. Residues were plotted with an 18-step, 5-turn output with the hydrophilic residues (VMCILYFW) indicated as blue squares, the hydrophobic residues (EDKRHQP NATSG) by black octagons, and the highly-hydrophobic substituted tryptophan (W; in relevant sequences) by a red diamond for clarity. All determinations of hydrophobicity/hydrophilicity were determined based upon the Wimley-White hydrophobicity index (Wimley & White, 1996). The wheels are arbitrarily bisected into the hydrophobic quadrant (B) (5/11 residues) and the hydrophilic quadrant (L) (11/12 residues).

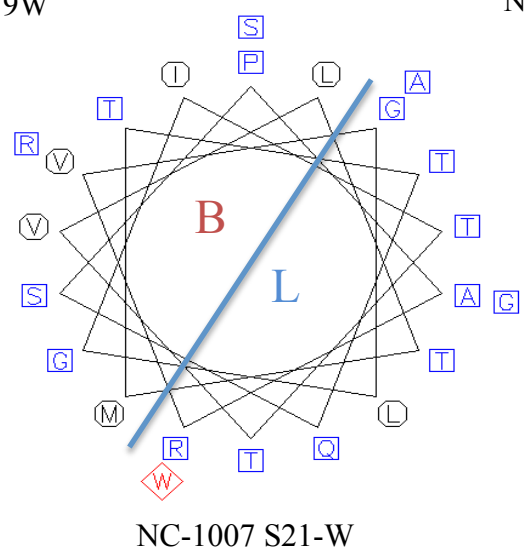
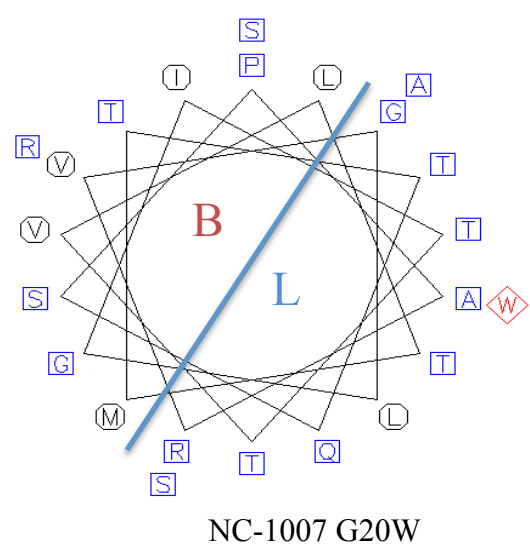
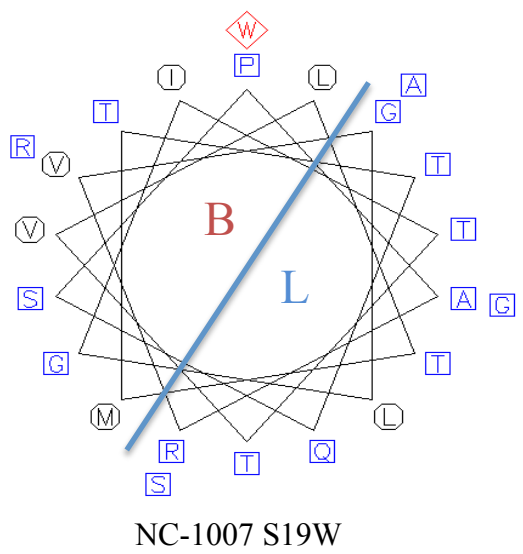
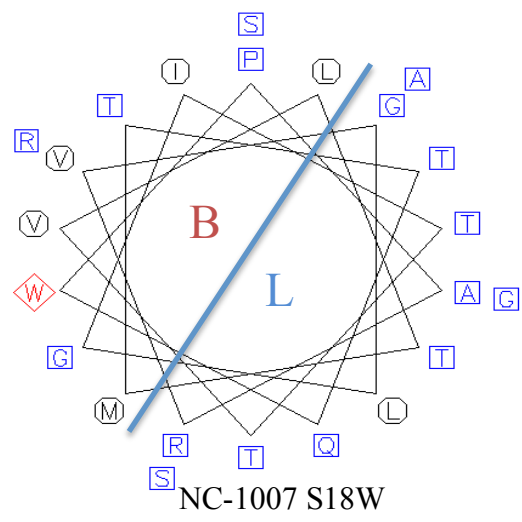
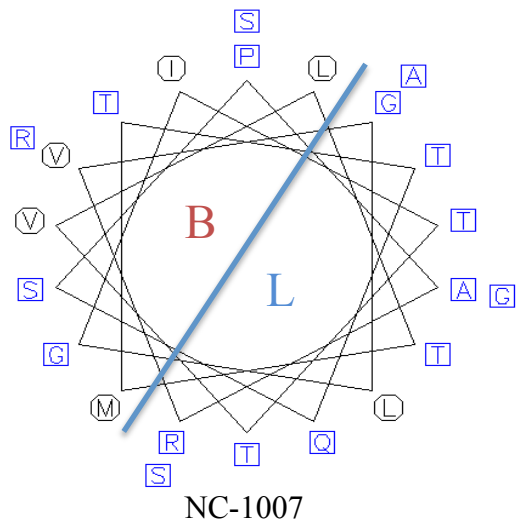


Figure 4.6 (opposite): Helix Wheel models of w-substituted NC1007 variants.

Helical wheel models are shown with hydrophilic residues highlighted in blue squares and hydrophobic residues noted in black circles. Red diamonds represent the location of the substituted tryptophan residue in the α -helix. Sequences are read beginning with the bottom residue at 12 o'clock (P in all presented cases), and following the connecting lines counterclockwise through the helix. The bisectonal divide represents approximations of the hydrophilic (L) and hydrophobic (B) faces of the helix.

All hydrophilicity/hydrophobicity data collected from the Wimley-White hydrophobicity index (Wimley & White, 1996).

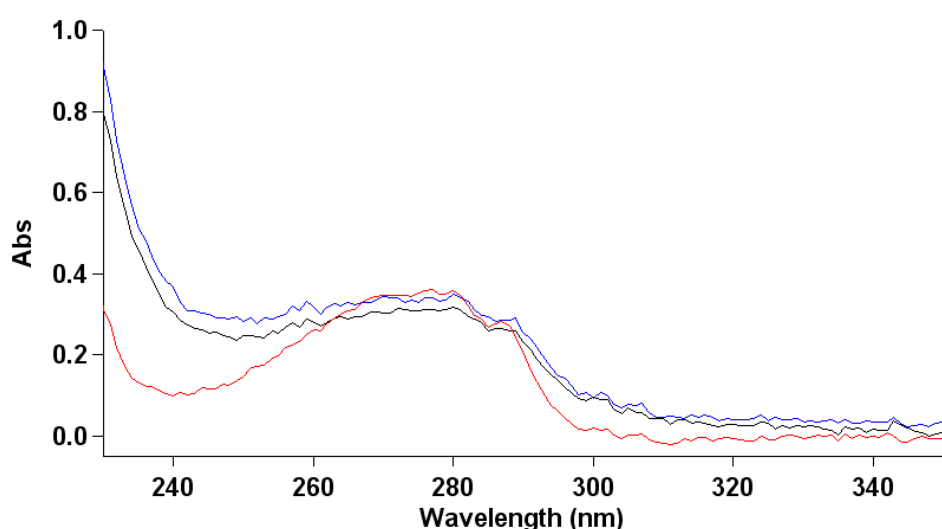


Figure 4.7 UV/Vis spectrophotometric profiles

Profile of free tryptophan (w; red), and its placement in the hydrophobic (NC1007 S18W; blue) or hydrophilic (NC1007 G20W; black) face of the transmembrane α -helix.

UV/Vis spectrometric profiles, when compared to free tryptophan in 50% TFE solution, demonstrate a merged peak including a violet shift, presumably caused by protection of tryptophan residues within the hydrophobic center of peptide aggregates. The effect was virtually identical regardless of the highly hydrophobic tryptophan residue's position in either the hydrophobic or hydrophilic face of the native peptide's α -helix. This suggests that at least some (and possibly all) aggregating peptide will orient such that the pore-defining tryptophan faces into the core of the aggregate, but roughly to the same extent regardless of position in the helix. The latter may be possible if the notable hydrophobic force of tryptophan is sufficient, even

when located among hydrophilic residues, to drive peptide orientation during aggregation such that it consistently faces inward. Extended studies into aggregate structure such as molecular modeling experiments will provide further evidence as to the mechanism behind aggregate peptide orientation.

In summary, although C-terminal tryptophan substitutions to NC1007 appeared to produce mild effects on kinetic parameters, the substitutions did little to reduce the propensity of the peptide to aggregate in solution and instead remain monomeric. This endpoint is vital from a drug-development perspective, and further study into the reduction of aggregation propensity in CK₄-M2GlyR peptides or the increase of NK₄-M2GlyR selectivity still shows potential leading to the development of a peptide capable of effectively and reliably serving as a replacement for defective ion channels in patients expressing, in particular Cl⁻ specific channelopathies, such as those which result in cystic fibrosis.

References

- Accurso, F. J., Rowe, S. M., Clancy, J. P., Boyle, M. P., Dunitz, J. M., Durie, P. R., Sagel, S. D., Hornick, D. B., Konstan, M. W., Donaldson, S. H., Moss, R. B., Pilewski, J. M., Rubenstein, R. C., Uluer, A. Z., Aitken, M. L., Freedman, S. D., Rose, L. M., Mayer-Hamblett, N., Dong, Q., Zha, J., Stone, A. J., Olson, E. R., Ordoñez, C. L., Campbell, P. W., Ashlock, M. A., & Ramsey, B. W. (2010). Effect of VX-770 in persons with cystic fibrosis and the G551D-CFTR mutation. *New England Journal of Medicine*, *363*(21), 1991-2003.
- Alexander, C., Ivetac, A., Liu, X., Norimatsu, Y., Serrano, J.R., Landstrom, A., Sansom, M., Dawson, D.C. (2009) Cystic fibrosis transmembrane conductance regulator: using differential reactivity toward channel-permeant and channel-impermeant thiol- reactive probes to test a molecular model for the pore. *Biochemistry*, *2048*(42), 10078- 10088.

- Anderson, M. P., Sheppard, D. N., Berger, H. A., & Welsh, M. J. (1992). Chloride Channels in the apical membrane of normal and cystic fibrosis airway and intestinal epithelia. *American Journal of Physiology*, 263(Pt 1), L1-14.
- Ashcroft, F. M. (2000). *Ion Channels and Disease*. San Diego, CA: Academic Press.
- Auld, D. S., Lovell, S., Thorne, N., Lea, W. A., Maloney, D. J., Shen, M., ... & Inglese, J. (2010). Molecular basis for the high-affinity binding and stabilization of firefly luciferase by PTC124. *Proceedings of the National Academy of Sciences*, 107(11), 4878-4883.
- Baer, M., Sawa, T., Flynn, P., Luehrsen, K., Martinez, D., Wiener-Kronish, J.P., Yarranton, G., Bebbington, C. (2009) An engineered human antibody Fab fragment specific for *Pseudomonas aeruginosa* PcrV antigen has potent anti-bacterial activity. *Infect Immun*. 77(3):1083-1090.
- Beck, E.J., Yang, Y., Yaemsiri, S., Raghuram, V. (2008) Conformational changes in a pore- lining helix coupled to cystic fibrosis transmembrane conductance regulator channel gating. *J Biol Chem*. 283: 4957-4966.
- Becq, J., Churlaud, C., & Deschavanne, P. (2010). A benchmark of parametric methods for horizontal transfers detection. *PLoS One*, 5(4), e9989.
- Bilton, D., Robinson, P., Cooper, P., Gallagher, C., Kolbe, J., Fox, H., Jaques, A., Charlton, B. (2011) Inhaled dry powder mannitol in cystic fibrosis: An efficacy and safety study. *Eur Respiratory J*. 38(5), 1071-1080.
- Boucher, R. C. (1994). Human airway ion transport, Part One. *American Journal of Respiratory and Critical Care Medicine*, 150(1), 271-281.
- Braun, P., von Heijne, G. (1999) The aromatic residues Trp and Phe have different effects on the positioning of a transmembrane helix in the microsomal membrane. *Biochemistry* 38, 9778-9782.
- Broughman, J.R., Mitchell, K.E., Iwamoto, T., Schultz, B.D., Tomich, J.M.. (2001). Amino-terminal modification of a channel forming peptide increases capacity for epithelial anion secretion. *American Journal of Physiology-Cell Physiology*, 280(3), C451-C458.
- Broughman, J.R., Shank, L.P., Takeguchi, W., Iwamoto, T., Mitchell, K.E., Schultz, B.D., Tomich, J.M. (2002). Distinct structural elements that direct solution aggregation and membrane assembly in the channel-forming peptide M2GlyR. *Biochemistry*, 41, 7350-7358.
- Broughman, J.R., Shank, L.P., Iwamoto, T., Prakash, O., Schultz, B.D., Tomich, J.M., Mitchell, K.E. (2002). Structural implications of placing cationic residues at either the NH₂- or COOH-terminus in a pore-forming synthetic peptide. *Journal of Membrane Biology*, 190, 93-103.
- Carpino, L. A., & Han, G. Y. (1972). 9-Fluorenylmethoxycarbonyl amino-protecting group. *The Journal of Organic Chemistry*, 37(22), 3404-3409.

- Cheer, S.M., Waugh, J., Noble, S. (2003) Inhaled tobramycin (TOBI): a review of its use in the management of *Pseudomonas aeruginosa* infections in patients with cystic fibrosis. *Drugs*, 63:2501-2520.
- Chen, X., Kube, D.M., Cooper, M.J., Davis, P.M. (2007) Cell Surface Nucleolin Serves as Receptor for DNA Nanoparticles Composed of Pegylated Polylysine and DNA. *Molecular Therapy* 16: 333–342.
- Clinicaltrials.gov
- Cook, G.A., Prakash, O., Zhang, K., Shank, L.P., Takeguchi, W.A., Robbins, A., Gong, Y.X., Iwamoto, T., Schultz, B.D., Tomich, J.M.. (2004) Activity and structural comparisons of solution associating and monomeric channel-forming peptides derived from the glycine receptor M2 segment. *Biophys J.* 86(3), 1424-1435.
- Costa, P. F., Emilio, M. G., Fernandes, P. L., Ferreira, H. G., & Ferreira, K. G. (1989). Determination of ionic permeability coefficients of the plasma membrane of *Xenopus Laevis* oocytes under voltage clamp. *The Journal of Physiology*, 413(1), 199-211.
- Cox, E. C., White, J. R., & Flaks, J. G. (1964). Streptomycin action and the ribosome. *Proceedings of the National Academy of Sciences of the United States of America*, 51(4), 703.
- Cressman, V. L., Hicks, E. M., Funkhouser, W. K., Backlund, D. C., & Koller, B. H. (1998). The Relationship of chronic mucin secretion to airway disease in normal and CFTR-deficient mice. *American Journal of Respiratory Cell and Molecular Biology*, 19(6), 853-866.
- Davis, P. B. (2006). Cystic Fibrosis Since 1938. *American Journal of Respiratory and Critical Care Medicine*, 173(5), 475-482.
- Demmers, J.A., van Duijn, E., Haverkamp, J., Greathouse, D.V., Koeppe, R.E. 2nd, Heck, A.J., Killian, J.A. (2001) Interfacial positioning and stability of transmembrane peptides in lipid bilayers studied by combining hydrogen/deuterium exchange and mass spectrometry. *J Biol. Chem.* 276, 34501-34508.
- de Planque, M.R., Bonev, B.B., Demmers, J.A., Greathouse, D.V., Koeppe, R.E. 2nd, Separovic, F., Watts, A. and Killian, J.A. (2003) Interfacial anchor properties of tryptophan residues in transmembrane peptides can dominate over hydrophobic matching effects in peptide-lipid interactions. *Biochemistry* 42, 5341-5348.
- Devidas, S., & Guggino, W. B. (1997). CFTR: domains, structure, and function. *Journal of Bioenergetics and Biomembranes*, 29(5), 443-451.
- Donaldson, S. H., Bennett, W. D., Zeman, K. L., Knowles, M. R., Tarran, R., & Boucher, R. C. (2006). Mucus clearance and lung function in cystic fibrosis with hypertonic saline. *New England Journal of Medicine*, 354(3), 241-250.
- Doyle, R. J., Chaloupka, J., & Vinter, V. (1988). Turnover of Cell Walls in microorganisms. *Microbiological Reviews*, 52(4), 554.

- Eckford, P. D., Li, C., Ramjeesingh, M., & Bear, C. E. (2012). CFTR potentiator VX-770 (ivacaftor) opens the defective channel gate of mutant CFTR in a phosphorylation-dependent but ATP-independent manner. *Journal of Biological Chemistry*, 287(44), 36639-36649.
- Edelhoch, H. (1967). Spectroscopic Determination of Tryptophan and Tyrosine in Proteins. *Biochemistry*, 6(7), 1948-1954.
- Elkins, M.R., Robinson, M., Rose, B.R., Harbour, C., Moriarty, C.P., Marks, G.B., Belousova, E.G., Xuan, W., Bye, P.T. (2006) A controlled trial of long-term inhaled hypertonic saline in patients with cystic fibrosis. *N Engl J Med*. 354:229-240.
- Fields, G. B., & Noble, R. L. (1990). Solid phase peptide synthesis utilizing 9-fluorenylmethoxycarbonyl amino acids. *International journal of peptide and protein research*, 35(3), 161-214.
- Frizzell, R. A., & Hanrahan, J. W. (2012). Physiology of epithelial chloride and fluid secretion. *Cold Spring Harbor Perspectives in Medicine*, 2(6).
- Fromter, E., & Diamond, J. (1972). Route of passive ion permeation in epithelia. *Nature New Biology*, 235(9), 13.
- Futaki, S. (1998). Peptide ion channels: design and creation of function. *Peptide Science*, 47(1), 75-81.
- Fuchs, H.J., Borowitz, D.S., Christiansen, D.H., Morris, E.M., Nash, M.L., Ramsey, B.W., Rosenstein, B.J., Smith, A.L., Wohl, M.E. (1994) Effect of aerosolized recombinant human DNase on exacerbations of respiratory symptoms and on pulmonary function in patients with cystic fibrosis. *N Engl J Med* 331:637-642.
- Goffeau, A., de Hertogh, B., & Baret, P. V. 2004. ABC Transporters. *Encyclopedia of Biological Chemistry. Vol. 1*, 1-5.
- Granseth, E., von Heijne, G., Elofsson, A. (2005) A study of the membrane-water interface region of membrane proteins. *J Mol. Biol.* 346(1), 377-385.
- Grasemann, H., Stehling, F., Brunar, H., Widmann, R., Laliberte, T.W., Molina, L., Doring, G., Ratjen, F. (2007) Inhalation of Moli1901 in patients with cystic fibrosis. *Chest* 131:1461-1466.
- Gstraunthaler, G. (2003). Alternatives to the use of fetal bovine serum: serum-free cell culture. *Altex*, 20(4), 275-281.
- Harzer, U., Bechinger, B. (2000) Alignment of lysine-anchored membrane peptides under conditions of hydrophobic mismatch: a CD, 15N and 31P solid-state NMR spectroscopy investigation. *Biochemistry* 39, 13106-13114.
- Higgins, C. F. (1995). The ABC of channel regulation. *Cell*, 82(5), 693-696.
- Hille, B. (2001). Ion channels of excitable membranes (Vol. 507). Sunderland, MA: *Sinauer*.

- Hong, H., Park, S., Jiménez, R.H., Rinehart, D., Tamm, L.K. (2007) Role of aromatic side chains in the folding and thermodynamic stability of integral membrane proteins. *J. Am. Chem. Soc.* 129(26), 8320-8327.
- Horisberger, J. D. (2003). ENaC–CFTR interactions: the role of electrical coupling of ion fluxes explored in an epithelial cell model. *Pflügers Archiv*, 445(4), 522-528.
- <http://investors.vrtx.com/releasedetail.cfm?releaseid=583683>
- <http://investors.vrtx.com/releasedetail.cfm?ReleaseID=856185>
- http://www.ptcbio.com/3.1.1_genetic_disorders.aspx
- Iwamoto, T., Grove, A., Montal, M. O., Montal, M., Tomich, J. M. (1994) Chemical synthesis and characterization of peptides and oligomeric proteins designed to form transmembrane ion channels. *International Journal of Peptide and Protein Research*, 43, 597-607.
- Jaques, A., Daviskas, E., Turton, J.A., McKay, K., Cooper, P., Stirling, R.G., Robertson, C.F., Bye, P.T., Lesouëf, P.N., Shadbolt, B., Anderson, S.D., Charlton, B. (2008) Inhaled mannitol improves lung function in cystic fibrosis. *Chest* 133(6): 1388–1396.
- Jayasinghe, S., Hristova, K., White S.H.(2001) Energetics, stability, and prediction of transmembrane helices. *J Mol Biol.* 312, 927-934.
- Jentsch, T. J., & Günther, W. (1997). Chloride channels: an emerging molecular picture. *Bioessays*, 19(2), 117-126.
- Jia, Y., Mathews, C. J., & Hanrahan, J. W. (1997). Phosphorylation by protein kinase C is required for acute activation of cystic fibrosis transmembrane conductance regulator by protein kinase *American Journal of Biological Chemistry*, 272(8), 4978-4984.
- Kim, D., & Steward, M. C. (2009). The role of CFTR in bicarbonate secretion by pancreatic duct and airway epithelia. *Journal of Medical Investigation*, 56(Supplement), 336-342.
- Konstan, M.W., Byard, P.J., Hoppel, C.L., Davis, P.B. (1995) Effect of high-dose ibuprofen in patients with cystic fibrosis. *N Engl J Med*, 332:848–854.
- Konstan, M.W., Davis, P.B., Wagener, J.S., Hilliard, K.A., Stern, R.C., Milgram, L.J.H., Kowalczyk, T.H., Hyatt, S.L., Fink, T.L., Gedeon, C.R., Oette, S.M., Payne, J.M., Muhammad, O., Ziady, A.G., Moen, R.C., Cooper, M.J. (2004) Compacted DNA nanoparticles administered to the nasal mucosa of cystic fibrosis subjects are safe and demonstrate partial to complete cystic fibrosis transmembrane regulator reconstitution. *Hum Gene Ther*, 15:1255–1269.
- Knowles, M., Gatzky, J., & Boucher, R. (1983). Relative ion permeability of normal and cystic fibrosis nasal epithelium. *Journal of Clinical Investigation*, 71(5), 1410.
- Kopito, R. R. (1999). Biosynthesis and degradation of CFTR. *Physiological reviews*, 79(1), S167-S173.

- Li, M., McCann, J. D., Anderson, M. P., Clancy, J. P., Liedtke, C. M., Nairn, A. C., Greengard, P., & Welsch, M. J. (1989). Regulation of chloride channels by protein kinase C in normal and cystic fibrosis airway epithelia. *Science*, *244*(4910), 1353-1356.
- Liedtke, C. M. (1989). Regulation of chloride transport in epithelia. *Annual review of physiology*, *51*(1), 143-160.
- Lowry, F. (2011) FDA Panel Sends Liprotamase Back to the Drawing Board. *Medscape Medical News*. <http://www.medscape.com/viewarticle/735722>
- Mach, H., Middaugh, C. R., & Lewis, R. V. (1992). Statistical determination of the average values of the extinction coefficients of tryptophan and tyrosine in native proteins. *Analytical Biochemistry*, *200*(1), 74-80.
- Mall, M., Grubb, B. R., Harkema, J. R., O'Neal, W. K., & Boucher, R. C. (2004). Increased airway epithelial Na⁺ absorption produces cystic fibrosis-like lung disease in mice. *Nature Medicine*, *10*(5), 487-493.
- McCarty, N. A. (2000). Permeation through the CFTR chloride channel. *Journal of Experimental Biology*, *203*(13), 1947-1962.
- Misfeldt, D. S., Hamamoto, S. T., & Pitelka, D. R. (1976). Transepithelial transport in cell culture. *Proceedings of the National Academy of Sciences*, *73*(4), 1212-1216.
- Mitaku, S., Hirokawa, T., Tsuji T. (2002) Amphiphilicity index of polar amino acids as an aid in the characterization of amino acid preference at membrane-water interfaces. *Bioinformatics* *18*, 608-616.
- Montal, M., Montal, M. S., & Tomich, J. M. (1990). Synporins--synthetic proteins that emulate the pore structure of biological ionic channels. *Proceedings of the National Academy of Sciences*, *87*(18), 6929-6933.
- Montal, M.O., Reddy, G.L., Iwamoto, T., Tomich, J.M., Montal, M. (1994) Identification of an ion channel-forming motif in the primary structure of CFTR, the Cystic Fibrosis Cl⁻ channel. *Proc. Natl. Acad. Sci. USA* *91*:1495-1499.
- Mutter, M., Hersperger, R., Gubernator, K., Müller, K. (1989) The construction of new proteins: V. A template-assembled synthetic protein (TASP) containing both a 4-helix bundle and beta-barrel-like structure. *Proteins*, *5*(1), 13-21.
- Norez, C., Antigny, F., Noel, S., Vandebrouck, C., & Becq, F. (2009). A cystic fibrosis respiratory epithelial cell chronically treated by miglustat acquires a non-cystic fibrosis-like phenotype. *American Journal of Respiratory Cell and Molecular Biology*, *41*(2), 217-225.
- Peltz, S. W., Welch, E. M., Jacobson, A., Trotta, C. R., Naryshkin, N., Sweeney, H. L., & Bedwell, D. M. (2009). Nonsense suppression activity of PTC124 (ataluren). *Proceedings of the National Academy of Sciences*, *106*(25), E64-E64.

- Pettit, R. S., & Johnson, C. E. (2011). Airway-rehydrating agents for the treatment of cystic fibrosis: past, present, and future. *Annals of Pharmacotherapy*, 45(1), 49-59.
- Pilewski, J. M., & Frizzell, R. A. (1999). Role of CFTR in airway disease. *Physiological reviews*, 79(1), S215-S255.
- Planells-Cases, R., & Jentsch, T. J. (2009). Chloride channelopathies. *Biochimica et Biophysica Acta (BBA)-Molecular Basis of Disease*, 1792(3), 173-189.
- Pollack, A. (2011) Vertex says trial of Vertex's VX-770, a cystic fibrosis drug, eased breathing. The Business of Health Care. Prescriptions Blog. *NYTimes.com*.
<http://prescriptions.blogs.nytimes.com/2011/02/23/vertex-says-cystic-fibrosis-drug-helped-patients-breathe-easier/>
- Quinton, P. M. (1999). Physiological basis of cystic fibrosis: a historical perspective. *Physiological reviews*, 79(1), S3-S22.
- Ray, W. A., Murray, K. T., Hall, K., Arbogast, P. G., & Stein, C. M. (2012). Azithromycin and the risk of cardiovascular death. *New England Journal of Medicine*, 366(20), 1881-1890.
- Reddy, G. L., Iwamoto, T., Tomich, J. M., & Montal, M. (1993). Synthetic peptides and four-helix bundle proteins as model systems for the pore-forming structure of channel proteins. II. Transmembrane segment M2 of the brain glycine receptor is a plausible candidate for the pore-lining structure. *Journal of Biological Chemistry*, 268(20), 14608-14615.
- Renna, M., Schaffner, C., Brown, K., Shang, S., Tamayo, M. H., Hegyi, K., ... & Floto, R. A. (2011). Azithromycin blocks autophagy and may predispose cystic fibrosis patients to mycobacterial infection. *The Journal of Clinical Investigation*, 121(121 (9)), 3554-3563.
- Reynolds, J. A., & Tanford, C. (1970). Binding of dodecyl sulfate to proteins at high binding ratios. Possible implications for the state of proteins in biological membranes. *Proceedings of the National Academy of Sciences*, 66(3), 1002-1007.
- Rice, P., Longden, I., & Bleasby, A. (2000). EMBOSS: The European Molecular Biology Open Software Suite. *Trends in Genetics*, 16(6), 276-277.
- Riordan, J. R. (2008). CFTR function and prospects for therapy. *Annual Review of Biochemistry*, 77, 701-726.
- Roccatano, D., Colombo, G., Fioroni, M., & Mark, A. E. (2002). Mechanism by which 2, 2, 2-trifluoroethanol/water mixtures stabilize secondary-structure formation in peptides: a molecular dynamics study. *Proceedings of the National Academy of Sciences*, 99(19), 12179-12184.
- Rowe, S. M., & Clancy, J. P. (2006). Advances in cystic fibrosis therapies. *Current opinion in pediatrics*, 18(6), 604-613.
- Rowntree, R. K., & Harris, A. (2003). The phenotypic consequences of CFTR mutations. *Annals of Human Genetics*, 67(5), 471-485.

- Saiman, L., Marshall, B. C., Mayer-Hamblett, N., Burns, J. L., Quittner, A. L., Cibene, D. A., ... & Macrolide Study Group. (2003). Azithromycin in patients with cystic fibrosis chronically infected with *Pseudomonas aeruginosa*: a randomized controlled trial. *Jama*, *290*(13), 1749-1756.
- Sagel, S.D., Sontag, M.K., Anthony, M.M., Emmett, P., Papas, K.A. (2011). Effect of an antioxidant-rich multivitamin supplement in cystic fibrosis. *J Cystic Fibrosis* *10*(1):31-36.
- Schmieden, V., Grenningloh, G., Schofield, P. R., & Betz, H. (1989). Functional expression in *Xenopus* oocytes of the strychnine binding 48 kd subunit of the glycine receptor. *The EMBO journal*, *8*(3), 695.
- Sears, H., Gartman, J., Casserly, P. (2011) Treatment options for cystic fibrosis: State of the art and future perspectives. *Reviews on Recent Clinical Trials* *6*(2): 94-107.
- Shank, L.P., Broughman, J.R., Brandt, R.M., Robbins, A.S., Takeguchi, W., Cook, G.A., Hahn, L., Radke, G., Iwamoto, T., Schultz, B.D., Tomich, J.M. (2006) Redesigning channel-forming peptides: amino acid substitutions in channel-forming peptides that enhance rates of supramolecular assembly and raise ion transport activity. *Biophys J.* *90*, 2138-2150.
- Sheppard, D. N., & Welsh, M. J. (1999). Structure and function of the CFTR chloride channel. *Physiological Reviews*, *79*(1), S23-S45.
- Sheridan, C. (2011) First cystic fibrosis drug advances towards approval. *Nature Biotechnology*, *29*(6): 465-466.
- Skou, J. C. (1998). The identification of the sodium–potassium pump (Nobel lecture). *Angewandte Chemie International Edition*, *37*(17), 2320-2328.
- Smith, J. J., Karp, P. H., & Welsh, M. J. (1994). Defective fluid transport by cystic fibrosis airway epithelia. *Journal of Clinical Investigation*, *93*(3), 1307.
- Stoikov, I. I., Antipin, I. S., & Konovalov, A. I. (2003). Artificial ion channels. *Russian chemical reviews*, *72*(12), 1055-1077.
- Tang, P., Mandal, P.K., Xu, Y. (2002) NMR structures of the second transmembrane domain of the human glycine receptor alpha(1) subunit: model of pore architecture and channel gating. *Biophys J.* *83*, 252-262.
- Tarran, R. (2004). Regulation of airway surface liquid volume and mucus transport by active ion transport. *Proceedings of the American Thoracic Society*, *1*(1), 42-46.
- Thibodeau, P. H., Richardson, J. M., Wang, W., Millen, L., Watson, J., Mendoza, J. L., Du, K., Fischman, S., Senderowitz, H., Lukacs, G. L., Kirk, K., & Thomas, P. J. (2010). The cystic fibrosis-causing mutation $\Delta F508$ affects multiple steps in cystic fibrosis transmembrane conductance regulator biogenesis. *Journal of Biological Chemistry*, *285*(46), 35825-35835.

- Tomich, J.M., Wallace, D.P., Henderson, K., Brandt, R., Ambler, C.A., Scott, A.J., Mitchell, K.E., Radke, G., Grantham, J. J. Sullivan, L.P., Iwamoto, T. (1998) Aqueous solubilization of transmembrane peptide sequences with retention of membrane insertion and function. *Biophysical Journal*. 74, 256-267.
- Tomich, J. M., Bukovnik, U., Layman, J., & Schultz, B. D. (2012). Channel Replacement Therapy for Cystic Fibrosis. *InTech - Open Access Publisher*. ISBN 979-953-307-059-8.
- van der Wel, P.C.A., Reed, N.D., Greathouse, D.V., Koeppe, R.E.II (2007) Orientation and motion of tryptophan interfacial anchors in membrane-spanning peptides. *Biochemistry* 46(25), 7514-7524.
- van Ginkel, F. W. Iwamoto, T., Schultz, B. D., & Tomich, J. M. (2008) Peptide-specific immunity to self-derived, anion channel-forming peptides in the respiratory tract. *Clinical and Vaccine Immunology*. 15(2): 260-266.
- Vogt, B., Ducarme, P., Schinzel, S., Brasseur, R., Bechinger, B. (2000) The topology of lysine-containing amphipathic peptides in bilayers by circular dichroism, solid-state NMR, and molecular modeling. *Biophys J*. 79, 2644-2656.
- Wallace, D.P., Tomich, J.M., Eppler, J., Iwamoto, T., Grantham, J.J., Sullivan, L.P. (2000) A Channel forming peptide induces Cl⁻ secretion by T84 cells: Modulation by Ca²⁺- dependent K⁺ channels. *Biochem Biophys Acta* 1464, 69-82.
- Wallace, D.P., Tomich, J.M., Iwamoto, T., Henderson, K., Grantham, J.J., Sullivan, L.P. (1997) A synthetic peptide derived from the glycine-gated Cl⁻ channel generates Cl⁻ and fluid secretion by epithelial monolayers. *Am J Physiol: (Cell Physiol)* 272: C1672- C1679.
- Wanner, A., Salathé, M., & O'Riordan, T. G. (1996). Mucociliary clearance in the airways. *American journal of respiratory and critical care medicine*, 154(6), 1868-1902.
- Welsh, M. J. (1987). Electrolyte transport by airway epithelia. *Physiological Reviews*, 67(4), 1143-1184.
- Wills, N. K., Reuss, L., & Lewis, S. A. (Eds.). (1996). Epithelial transport: a guide to methods and experimental analysis. *Springer*.
- Wilschanski, M., Miller, L., Shoseyov, D., Blau, H., Rivlin, J., Aviram, M., Cohen, M., Armoni, S., Yaakov, Y., Pugatch, T., Cohen-Cymerknoh, M., Miller, N.L., Reha, A., Northcutt, V.J., Hirawat, S., Donnelly, K., Elfring, G.L., Ajayi, T., Kerem, E. (2011) Chronic ataluren (PTC124) treatment of nonsense mutation cystic fibrosis. *Eur Respiratory J*. 38(1): 59-69.
- Wimley, W. C., & White, S. H. (1996). Experimentally determined hydrophobicity scale for proteins at membrane interfaces. *Nature Structural Biology*, 3(10), 842-848.
- Yushmanov, V.E., Mandal, P.K., Liu, Z., Tang, P., Xu, Y. (2003) NMR structure and backbone dynamics of the extended second transmembrane domain of the human neuronal glycine receptor $\alpha 1$ subunit. *Biochemistry* 42, 3989-3995.



Zhang, Z. R., McDonough, S. I., & McCarty, N. A. (2000). Interaction between permeation and gating in a putative pore domain mutant in the cystic fibrosis transmembrane conductance regulator. *Biophysical Journal*, 79(1), 298-313.

Zhou, Z., Hu, S., Hwang, T.C. (2002) Probing an open CFTR pore with organic anion blockers. *J Gen Physiol.* 120:647-662.

Appendix A - Rights and Permissions

Rightslink® by Copyright Clearance Center

https://s100.copyright.com/AppDispatchServlet

HomeCreate AccountHelp Live Chat

 **ACS Publications** Title: Distinct Structural Elements That Direct Solution Aggregation and Membrane Assembly in the Channel-Forming Peptide M2GlyR†
Most Trusted. Most Cited. Most Read.

Author: James R. Broughman, Lalida P. Shank, Wade Takeguchi, et al
Publication: Biochemistry
Publisher: American Chemical Society
Date: Jun 1, 2002
Copyright © 2002, American Chemical Society

User ID

Password

Enable Auto Login

LOGIN

[Forgot Password/User ID?](#)
If you're a **copyright.com user**, you can login to RightsLink using your copyright.com credentials. Already a **RightsLink user** or want to [learn more?](#)

PERMISSION/LICENSE IS GRANTED FOR YOUR ORDER AT NO CHARGE

This type of permission/license, instead of the standard Terms & Conditions, is sent to you because no fee is being charged for your order. Please note the following:

- Permission is granted for your request in both print and electronic formats, and translations.
- If figures and/or tables were requested, they may be adapted or used in part.
- Please print this page for your records and send a copy of it to your publisher/graduate school.
- Appropriate credit for the requested material should be given as follows: "Reprinted (adapted) with permission from (COMPLETE REFERENCE CITATION). Copyright (YEAR) American Chemical Society." Insert appropriate information in place of the capitalized words.
- One-time permission is granted only for the use specified in your request. No additional uses are granted (such as derivative works or other editions). For any other uses, please submit a new request.

If credit is given to another source for the material you requested, permission must be obtained from that source.

BACK

CLOSE WINDOW

Copyright © 2014 [Copyright Clearance Center, Inc.](#) All Rights Reserved. [Privacy statement.](#) Comments? We would like to hear from you. E-mail us at customercare@copyright.com

1 of 1

11/19/14, 9:29 PM

All other content has open access permission under a creative commons license.